

THE ASEAN JOURNAL OF RADIOLOGY

January - April 2011
Volume XVII Number I
ISSN 0859 144X

8th AOCNR 2011

ASIAN OCEANIAN CONGRESS
OF NEURO-RADIOLOGY

OCTOBER 26-28, 2011
Shangri-la Hotel **Bangkok, THAILAND**

Supported by



AOSNHNR
Asian &
Oceanian
Society of
Neuroradiology
and
Head & Neck
Radiology

Organized by



www.AOCNR2011.com

Published by
Royal College of Radiologists of Thailand

and

Radiological Society of Thailand
Bangkok, Thailand.

Welcome Message

Dear Colleagues,

On behalf of the Neuroradiological Association of Thailand and the Organizing Committee of the 8th Asian Oceanian Congress of Neuroradiology, I would like to extend a warm welcome to all participants to the 8th AOCNR Conference in Bangkok, Thailand.



The Organizing Committee of the 8th AOCNR has prepared the Scientific Program that will cover a wide spectrum of topics as far reaching as those related to specific problems affecting our own region to those that pertain to advanced knowledge and technical bases in the fields of Neuroradiology as well as Head and Neck Radiology. As we all aware of rapid progress, advancement and development in these fields, it is our obligation to exchange expertise and broadly disseminate the continuing achievements in knowledge and technologies among our colleagues.

The Programs will thus focus on educational lectures, symposia and interactive sessions by experts in the fields of Neuroradiology including Interventional Neuroradiology, and Head and Neck Radiology. There will be a broad and exciting panel of distinguished lecturers, discussions and seminars, as well as awards given to participants to encourage ongoing scientific research.

The Asian and Oceanian Society of Neuroradiology and Head & Neck Radiology (AOSNHNR) was founded in 1994 with Professor Mutsumasa Takahashi serving as its first President. Through his inspired leadership and efforts, the first Asian and Oceanian Congress of Neuroradiology and Head & Neck Radiology (AOCNHNR) was held in Kumamoto, Japan. The Society has continued to grow with many new member countries.

The name of the Congress was shortened to the Asian Oceanian Congress of Neuroradiology (AOCNR) in 2007. The Congresses were held every 3-4 years originally, and now every 2 years in various Asian and Oceanian countries with the aim of promoting Neuroradiology and Head and Neck Radiology in the region. The last AOCNR Conference, its 7th, was conducted with great success in Bali, Indonesia in 2009.

We hope that the 8th AOCNR Conference will afford participants great opportunities to share their scientific knowledge, as well as to meet each other in a stimulating social and academic setting filled with abundant activities to strengthen our fields and our friendships.

We are also certain that you will have the chance to experience some of Thailand's many attractions, culture and our world famous cuisine.

Nitaya Suwanwela

Professor of Radiology

Congress Chair



Welcome Message

Dear Friends and Colleagues



On behalf of the Secretary General of 8th AOCNR , I warmly welcome all participants to 8th AOCNR in Bangkok, Thailand.

The Organizing Committee of the 8th AOCNR has prepared all the possible best including events this congress the Scientific Program that will cover a wide spectrum of topics as far reaching as those related to specific problems affecting our own region to those that pertain to advanced knowledge and technical bases in the fields of Neuroradiology as well as Head and Neck Radiology. As we all aware of rapid progress, advancement and development in these fields, it is our obligation to exchange expertise and broadly disseminate the continuing achievements in knowledge and technologies among our colleagues. Above from the scientific sessions, The warmest welcome and hospitality are provided through our the three days meeting, as well as all the social and AOSNHNR executive committee meeting

I wish to thank organizing committee for their efforts in ringing this meeting to fruition and I would like to thank sponsors and exhibitors for their support and contribution in making this meeting successful. Special thanks also go to the delegates and everyone involved in the meeting.

Sirintara Pongpech, M.D.

Secretary General of 8th AOCNR

Message from the Scientific Chair



From its inception in 1994 at Kumamoto (Japan), AOCNR congresses have been the venue of exchange and updated knowledge in the field of diagnostic neuroimaging and neurointervention among the radiologists, technologists, scientists and healthcare personnel in related field in Asia and Oceania regions as has been inspired by the late Professor M. Takahashi, the pioneer of the AOSNHNR and finally the AOCNR.

This 8th AOCNR 2011 in Bangkok has provided the mixtures of lectures and interactive sessions in imaging of the brain, head and neck, spines and neurointervention. The contents of the presentation are composed of both updated fundamental knowledge that we are using on the daily practice and the new and advanced frontier knowledge in the field. The lectures are delivered by the leaders in the field from all over the world who are willing to teach and to share. Follow the lectures, the related interactive cases presentation will take us back to the real cases that we have to face with. The leaders of the sessions will take us through the thinking process in solving the problems and get the pertinent information to help the clinicians managing the cases.

In addition, the electronic poster presentation sessions will allow us to share and discuss the research experience among friends. Several awards provided for the selected papers are generous and give the equal opportunity for several categories of research to allow varieties of work to be acknowledged.

I hope that all of us attending the congress feel the hospitality and enjoy the academic ambience we provided. Have fun and enjoy.

Jiraporn Laothamatas, M.D.



Organizing Committee 8th AOCNR

Executive Organizing Committee

Congress Chair	Nitaya Suwanwela
Vice Chairman	Suthisak Suthipongchai
Secretary General	Sirintara Pongpech
Scientific Program	Jiraporn Laothamatas
Finance and Fund Raising	Suthisak Suthipongchai
Treasurer	Anchalee Churojana
Social	Pakorn Jiarakongmun
Publications	Orasa Chawalparit
	Warinthorn Phuttarak
Web Master	Anek Suwanbundit
	Chaleumpon Tachawisate
Secretariat	Pakorn Jiarakongmun
	Yothin Kunsang

Regional Advisory Committee

Elizabeth Thompson	Australia
Mark Soo Yoison	Australia
Michael Sage	Australia
Lin Ma	China
Dai Jian-Ping	China
Wong Yiu Chung	Hong Kong SAR
Lilian Leong	Hong Kong SAR
Rajesh Kapur	India
Benny Huwae	Indonesia
Donny Melita	Indonesia
Sri Andreani Utomo	Indonesia
Darioush Etemadi	Iran
Kazuhiro Katada	Japan
Kazuhiro Tsuchiya	Japan



Regional Advisory Committee (cont.)

Yukumori Korogi	Japan
Sang Joon Kim	Korea
Kim Dong-Ik	Korea
Gyung-Ho Chung	Korea
Adam Pany	Malaysia
Valarmathi Subramaniam	Malaysia
Sobri Muda	Malaysia
Lin Tun Tun	Myanmar
David Perry	New Zealand
Umar Rashid Chaudhry	Pakistan
Muhammad Nawaz	Pakistan
Benjamin Adapon	Philippines
Henry Adapon	Philippines
P.Maryjo Sarino	Philippines
Fahad Al Qahtani	Saudi Arabia
Jehad Al Watban	Saudi Arabia
Mohamed Aabed Al Thagafi	Saudi Arabia
Francis Hui	Singapore
Vincent Chong	Singapore
Tchoyoson Lim	Singapore
A.N.I. Wijesinha	Sri Lanka
Adel Shannan	Syria
Said Houaja	Syria
Wan-Yuo Guo	Taiwan
Michael Teng Mu-Huo	Taiwan
Sandy Chen	Taiwan
Nitaya Suwanwela	Thailand
Sirintara Pongpech	Thailand
Suthisak Suthipongchai	Thailand
Hoang Duc Kiet	Vietnam

**Scientific Committee 8th AOCNR**

Jiraporn Laothamatas

Sukalaya Lerdlum

Orasa Chawalparit

Anchalee Churojana

Lojana Tuntiyatorn

Pantip Suwansaard

Panreuthai Trinavarat

Dittapong Songsaeng

Ratana Kuntiranon

Ekachat Chanthanaphak

Thanwa Sudsang



The Committee of Royal College of Radiologists of Thailand

Apr 2011-Mar 2013

President:	Permyot	Kosolbhand
Vice-president:	Sirintara	Singhara Na Ayudya
Secretariat General:	Pongdej	Pongsuwan
Vice-secretary General:	Alongkorn	Kiatdilokrath
Treasurer:	Krisdee	Prabhassawat
Academic president:	Anchalee	Churojana
House Master & Social Programme:	Kiat	Arjhansiri
Secretary:	Vithya	Varavithya
Registrar:	Pisit	Wattanuakongkorn
Committee:	Poonsook	Jitnusun
	Chamaree	Chuapatcharasopon
	Chantima	Rongviriyapanich
	Nitra	Piyaviseipat

The Committee of Radiological Society of Thailand

Apr 2011-Mar 2013

President:	Permyot	Kosolbhand
Vice-president:	Sirintara	Singhara Na Ayudya
Secretariat General:	Pongdej	Pongsuwan
Treasurer:	Krisdee	Prabhassawat
Academic president:	Anchalee	Churojana
House Master&Social Programme:	Kiat	Arjhansiri
Committee:	Poonsook	Jitnusun
	Chamaree	Chuapatcharasopon
	Chantima	Rongviriyapanich
	Nitra	Piyaviseipat
	Amphai	Uraiverotchanakorn



The Journal of the Royal College of Radiologists & Radiological Society of Thailand (2011 - 2013)

- Editor:** Sirintara (Pongpech) Singhara Na Ayudya
- Co-Editor:** Permyot Kosolbhand
- Editorial board:**
- | | |
|------------------------|---------------------------|
| Poonsook Jitnusun | Anchalee Churojana |
| Walailak Chaiyasoot | Jitladda Wasinrat |
| Dittapong Songsaeng | Kriengkrai Iemsawatdikul |
| Nitra Piyaviseipat | Numphung Numkarunaranrote |
| Monravee Tumkosit | Sith Phongkitkarun |
| Chanika Sritara | Putipun Puataweepong |
| Thanwa Sudsang | Suwalee Pojchmarnwiputh |
| Sirianong Namwongprom | Ekkasit Taravijitkul |
| Jiraporn Srinakarin | Jureerat Thammaroj |
| Wiwatana Tanomkiat | Siriporn Hirunpatch |
| Busabong Noola | Kamolwan Jungmeechoke |
| Anuchit Reumthantong | Wichet Piyawong |
| Kaan Tangtiang | Wananee Meennuch |
| Wittaya Prasitvoranant | |
- Emeritus Editors:** Kawee Tungsubutra
Poonsook Jitnusun

Office:

1. Department of Radiology, Faculty of medicine, Ramathibodi hospital 270, Rama VI Road, Toong Phayathai, Ratchathewi, Bangkok, 10400
Tel 02-2011259#110, Fax 02-2011297
E-mail Sirintarapongpech2@hotmail.com
2. The Royal college of Radiologists & Radiological society of Thailand, 9th Floor, Royal Golden Jubilee Building, 2 Soi Soonvijai, Petchburi Road, Bangkok, 10320
Tel 02-7165963, Fax 02-7165964
E-mail rcrthailand@gmail.com



SCIENTIFIC PROGRAM

October 26, 2011

7.00	Registration : Area R	
	8.00-10.00: Grand Ballroom	
	Chairman: Nitaya Suwanwela Co-chairman: Sirintara Pongpech	
08.00 - 08.30	Opening Remarks	
	Welcome Speech: Benny Huwae, Indonesia Nitaya Suwanwela, Thailand	
08.30 - 08.40	Keynote Speech	
	AOSNR and Takahashi Foundation Mutsumasa Takahashi, Japan	
08.40 - 09.20	Takahashi Honorable Lecture	
	The New WHO Classification of CNS Neoplasms, Update 2011: What can the neuroradiologist really say? Anne G. Osborn, USA	
09.20 - 10.00	AOCNR Symposium 1	
	Imaging of the Temporal Bones: Key Issues 2011 Hugh D. Curtin, USA	
	10.00-10.30: Area E	
	Break /Scientific Exhibit Opening: Mutsumasa Takahashi	
	Chairman: Pakorn Jiarakongmun	
	10.30-12.10: Grand Ballroom	
	Room 1 : Brain Tumor	Room 2 : Head and Neck
	Chairman: Yukunori Korogi Co-chairman: Thanwa Sudsang	Chairman: A.N.I Wijesinha Co-chairman: Dittapong Songsaeng
10.30 - 11.00	CNS Glial Cell Tumors Anne G. Osborn, USA	Imaging of Nasopharyngeal Cancer and Its Pattern of Spread Vincent Chong, Singapore
11.00 - 11.40	Interactive Session: Brain Tumor Ratana Kunnatiranont, Thailand Punjama Lertbutsayanukul, Thailand	Interactive Session: Head and Neck Anchalee Churojana, Thailand Pantip Suwansaard, Thailand
11.40 - 12.10	Imaging of CNS Lymphoma and Its Variants Anne G. Osborn, USA	Imaging of the Larynx: Key Points and Pitfalls 2011 Hugh D. Curtin, USA
	12.10-13.30: Grand Ballroom	
	Luncheon Symposium : The New Technology of the Treatment of Ischemic Stroke (Manish Taneja, MD, FRCR, FAMS)	
	13.30-15.50: Grand Ballroom	
	Room 1	
	Chairman: Jiraporn Laothamatas Co-chairman: Oranan Tritanon	
13.30 - 14.10	AOCNR Symposium 2 Update in Dementia Imaging Stefan Sunaert, Belgium	
	Room 1 : Dementia	Room 2 : Head and Neck
		Chairman: Kitima Thammarak Co-chairman: Warinthorn Phuttharak
14.10 - 14.40	Imaging of Dementia: Neurodegenerative Change Stefan Sunaert, Belgium	Imaging of the Neck Nodes: What is the Significance? Hugh D. Curtin, USA
14.40 - 15.20	Interactive Session: Dementia and Neurodegenerative Diseases Nicolas Trost, Australia Dittapong Songsaeng, Thailand	Interactive Session: Temporal Bone and Orbit Pailin Kongmebhoh, Thailand Netsiri Dumrongpisutikul, Thailand
15.20 -15.50	Cerebral Disease of Iron Mark A. van Buchem, Netherlands	Imaging of Orbital Neoplasms Sukalaya Lerdium, Thailand
	15.50-16.10: Area E	
	Break / Poster Presentation 1-3	
	Chairman: Orasa Chawalparit Co-chairman Pailin Kongmebhoh	
	16.10-17.30: Grand Ballroom	
	Chairman: Pailin Kongmebhoh Co-chairman: Punjama Lertbutsayanukul	
16.10 - 16.50	AOCNR Symposium 3 Post-treatment Imaging of Head and Neck Cancer Hugh D. Curtin, USA	
16.50 - 17.30	AOCNR Symposium 4 Cerebral Small Vessel Disease from an Imaging Perspective Mark A. van Buchem, Netherlands	
19.00 - 21.00	Gala Dinner: Grand Ballroom	



October 27, 2011

8.00-10.00: Grand Ballroom		
	Room 1	
	Chairman: Nicholas Trost Co-chairman: Kittisak Unsrisong	
08.00 - 08.40	AOCNR Symposium 5 Neurological Applications of Diffusion Imaging and DTI Stefan Sunaert, Belgium	
	Room 1 : Advanced Imaging	Room 2 : Spine
		Chairman: Lin Tun Tun Co-chairman: Wiboon Suriyajakruththana
08.45 - 09.20	7Tesla MRI: Early Experience in Brain Imaging Mark A. van Buchem, Netherlands	Concept of Imaging in Degenerative Spine Ron Shnier, Australia
09.20 - 10.00	Interactive Session: Perfusion Imaging Kazuhiro Katada, Japan Thanwa Sudsang, Thailand	Interactive Session: Spine: Degenerative Disease Siri-on Tritrakarn, Thailand
	10.00-10.30: Area E	
	Break/ Poster Presentation 4-6	
	Moderator: Chewarat Wirojtananagoon	
	10.30-12.00: Grand Ballroom	
	Room 1 : Advanced Imaging	Room 2 : Spine
	Chairman: Ratana Kuntiranon Co-chairman: Chewarat Wirojtananagoon	Chairman: Jureerat Thammaroj Co-chairman: Kittipong Riabroi
10.30 - 11.00	Clinical Applications of CT Perfusion in Neuroimaging Kazuhiro Katada, Japan	Inflammatory and Demyelinating Disease of the Spinal Cord Orasa Chawalparit, Thailand
11.00 - 11.30	fMRI and Its Clinical Applications: Theory and How to Stefan Sunaert, Belgium	Imaging of Spinal Tumor Anne G. Osborn, USA
11.30 - 12.00	Tips, Tricks and Pitfalls in Clinical DTI Kei Yamada, Japan	Stem Cell Therapy in Spinal Cord Injury Ron Shnier, Australia
	12.00-13.20: Grand Ballroom	
	Luncheon Symposium	
	13.20-14.40: Grand Ballroom	
	Chairman: Jehad Al Watban , Co-chairman: Lojana Tuntiyatorn	
13.20 - 14.00	AOCNR Symposium 6 The Aging Brain: Imaging Aspects Mark A. van Buchem, Netherlands	
14.00 - 14.40	AOCNR Symposium 7 MRI of the Spine - Spectrum of Diseases and Problem Solver Ron Shnier, Australia	
	14.40-15.10: Area E	
14.40 - 15.10	Break/ Poster Presentation 7-9	
	Moderator: Punjama Lertbutsayanukul	
	15.10-17.40: Grand Ballroom	
	Room 1 : Advanced Imaging	Room 2 : Spine
	Chairman: Nasuda Danchaivichit Co-chairman: Jiraporn Laothamatas	Chairman: Pipat Chiewvit Co-chairman: Warinthorn Phuttharak
15.10 - 15.40	Neurological Applications of MR Spectroscopy Jiraporn Laothamatas, Thailand	Imaging of Spinal Infection Jureerat Thammaroj, Thailand
15.40 - 16.20	Interactive Session: MR Spectroscopy Chang Kee-Hyun, Korea Lojana Tuntiyatorn, Thailand	Interactive Session: Spine: Infection and Inflammation Warinthorn Phuttharak, Thailand Chewarat Wirojtananagoon, Thailand
16.20 - 17.00	AOCNR Symposium 8 Imaging of Post-operative Spine and Failed Back Syndrome Jiraporn Laothamatas, Thailand	
17.00 - 17.40	AOCNR Symposium 9 Noninvasive Spinal Vascular Imaging Karel Ter Brugge, Canada	

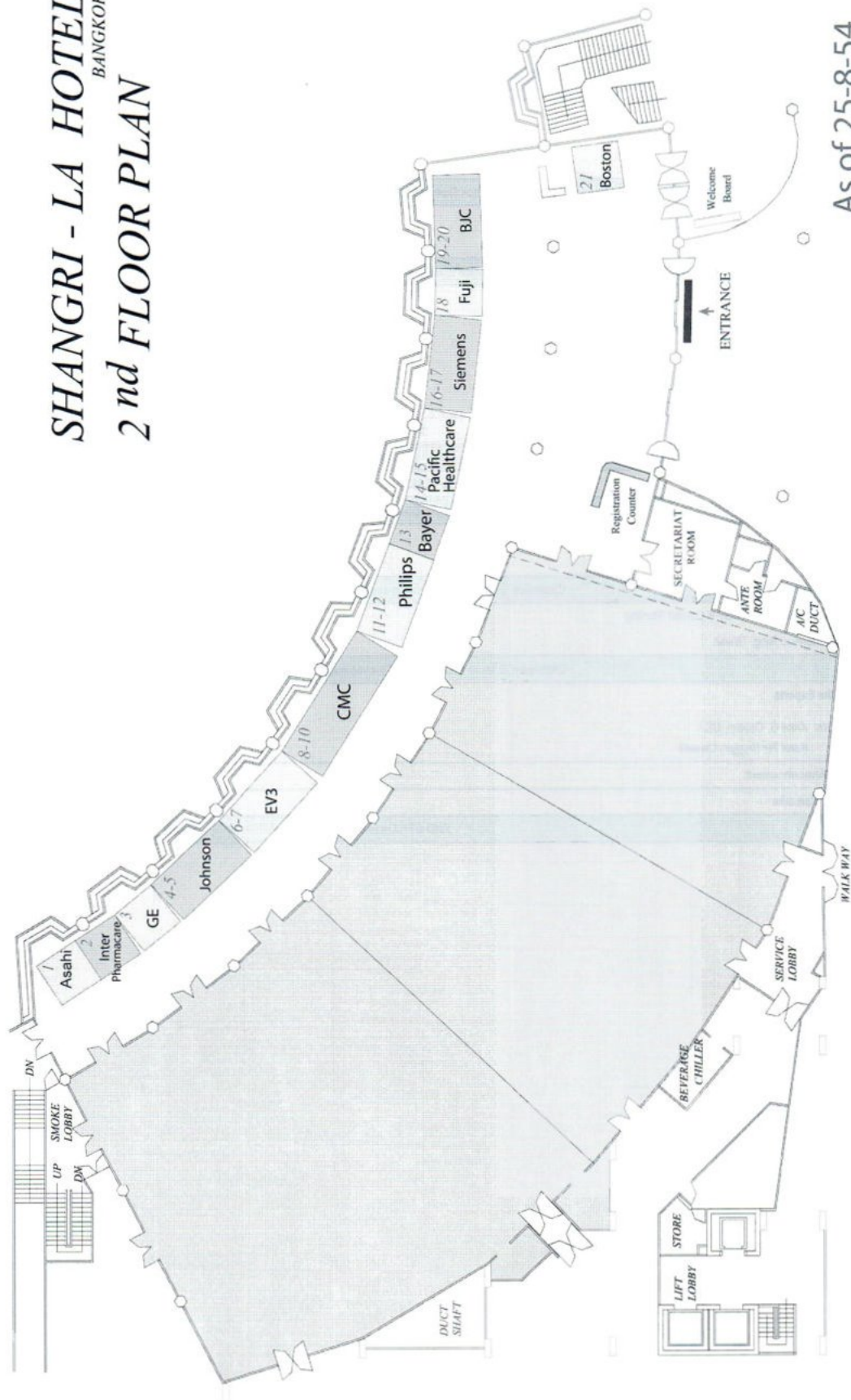


October 28, 2011

8.00-10.00: Grand Ballroom	
8.00 -8.45	Chairman: Suthisak Suthipongchai Co-chairman: Francis Hui
	Pierre Lasjaunias Honorable Lecture Arterial Wall Vasculopathies and Imaging Correlation <i>Karel Ter Brugge, Canada</i>
8.45 - 9.15	Chairman: Jarturon Tantivatana Co-chairman: Kittisak Unsrirong
	Update in Aneurysmal Treatment <i>In Sup Choi, USA</i>
9.15 - 10.00	Chairman: Anchalee Churojana Co-chairman: Sirintara Pongpech
	Panel Discussion Traumatic Vascular Lesions in the Region <i>Panelists : Coung T.C., Vietnam</i> <i>Sabri Muda, Malaysia</i> <i>Anchalee Churojana, Thailand</i>
10.00-10.15	
Break	
10.15-12.45: Grand Ballroom	
10.15-10.45	Chairman: Henry Adapon Co-chairman: Pakorn Jiarakongmun
	Dural Arteriovenous Shunts: from Diagnosis to Treatment <i>Dong Joon Kim, Korea</i>
10.45-11.15	Chairman: Sri Andreani Utomo Co-chairman: Dittapong Songsaeng
	The Value of Perfusion Study in Carotid Stenting <i>Michael Mu-Huo Teng, Taiwan</i>
11.15-12.30	Chairman: Jiraporn Laothamatas Co-chairman: Sirintara Pongpech
	Meet the Experts <i>Panelists: Anne G. Osborn, USA</i> <i>Karel Ter Brugge, Canada</i>
12.30-12.45	Award Announcement
	Closing Remarks
END OF CONGRESS	



SHANGRI - LA HOTEL BANGKOK 2nd FLOOR PLAN





Keynote Speech

Mutsumasa Takahashi M.D.

Education and Training:

- 1960 Kyushu University School of Medicine
- 1962 University of Michigan Hospital, Residency in Radiology
- 1965 Stanford University Hospital, Fellowship in Cardiovascular Radiology
- 1966 UCLA Hospital, Fellowship in Neuroradiology

Staff Appointments

- 1972 Akita University School of Medicine, Professor and Chairman
- 1977 UCLA, Visiting Professor in Radiology
- 1980 Kumamoto University School of Medicine, Professor and Chairman
- 2001 Secom Teleradiology Service, Director
- 2007 Ugatake Hospital, Imaging Center, Director
- 2011 Nishinihon Hospital, Radiology, Director

Presidents of Scientific Meetings

- 1983 13th Japanese Society of Neuroradiology, Tokyo
- 1994 XV Symposium Neuroradiologicum, Kumamoto
- 2000 XV International Society of Head and Neck Radiology, Kumamoto
- 2000 59th Japanese Society of Radiology, Yokohama
- 2004 12th International Society of Magnetic Resonance in Medicine, Kyoto

Honors and Awards

Honorary Members and Fellowships

RSNA, Chinese Society of Radiology, American College of Radiology, European Society of Radiology, French Society of Radiology, Royal College of Radiologists, American Society of Neuroradiology, Japanese Society of Radiology

Awards;

- 2001 Gold Medal, RSNA
- 2004 Beclere Medal, International Society of Radiology



Imaging of the Larynx: Key Points and Pitfalls 2011

Hugh D. Curtin, M.D.

*Massachusetts Eye and Ear Infirmary, Harvard Medical School
Boston, MA, USA*

Introduction

Squamous cell carcinoma of the larynx is almost always detected by direct visualization. Imaging is used to determine extent of the primary tumor and to look for nodal metastasis. Current therapy includes many surgical options as well as radiation and radiation/ chemotherapy protocols. Surgery can be used to salvage cases with recurrence after non-surgical protocols. Surgery includes total laryngectomy and various voice sparing partial laryngectomies. Recent surgical advances include accomplishment of endoscopic partial resections and extended partial laryngectomies. Lasers are now used not only as cutting instruments and also in also as angiolytic tools.

The information gathered by imaging applies to patients that are candidates for any of the therapeutic options. If one focuses on the landmarks needed for voice sparing partial laryngectomies, comments on the volume of the primary, and looks at the nodes then all those involved with therapy planning should have the information that they need. CT and MRI are the primary imaging approaches to definition of the anatomy. Recently PET scanning has been used to help predict outcome of various therapies.

The most important landmarks are the laryngeal ventricle, the upper edge of the cricoid and the crico-arytenoid joint. The status of the cartilage is under increasing scrutiny as the implications of various findings to therapeutic outcomes are explored.

Imaging laryngeal Squamous Cell CA

At our institution, we begin imaging larynx carcinoma with contrast enhanced CT. The speed and resolution of CT allows the radiologist to answer almost all important questions. Currently we use collimation of 1 mm or less but reconstruct images of 2 to 3 mm in axial and coronal planes.

We currently use magnetic resonance only as a limited study and only if there is a question after CT scanning. The usual indication is a persistent question about invasion of the cartilage or occasionally there is a need to assess the margin between the tumor and the thyroarytenoid muscle. Some investigators prefer MRI for the initial evaluation. Changes occur with each new iteration of technology.



After therapy we follow with contrast enhanced CT but are beginning to use PET/CT more routinely or when there is ambiguous soft tissue seen on the scan. Activity in the muscles at PET can lead to confusion.

Submucosal lesions

Submucosal lesions are a different issue. Here the otolaryngologist sees a mucosal bulge but the diagnosis not known. The radiologist can often give an exact diagnosis. Most lesions are chondrosarcomas or laryngoceles (saccular cysts). A laryngocele is a dilation of the small ventricular appendix which extends superiorly from the ventricle into the supraglottic paraglottic space. Submucosal solid tumors other than chondrosarcomas are rare.



Imaging of the Neck Nodes: What is the significance?

Hugh D. Curtin MD

*Massachusetts Eye and Ear Infirmary, Harvard Medical School
Boston, MA, USA*

Introduction

The status of the nodes in a patient with squamous cell cancer (SCCa) of the head and neck is a very important prognostic indicator. The presence of tumor in a single lymph node diminishes the chance of survival by one half. Tumor extending through the capsule of a node further diminishes the chance of survival. The significance of nodal disease in thyroid carcinoma is significantly less than in SCCa.

Squamous cell carcinoma (SCCa)

Imaging of the neck nodes is performed for initial staging. More recently imaging has been used to predict and to follow response to non surgical therapies.

Initial staging

For pre-therapeutic imaging, the first task is to determine if there is or is not a positive node. Is the neck radiologically positive (rN+) or is the neck radiologically negative (rN0). There are several strategies but there are limitations to all.

The size criteria we use are 1.5cm in the submental/submandibular spaces (level I) and the upper jugular region (Level II) and 1cm in other levels. For the node of Rouviere many suggest 8mm as a maximum. An internal architectural abnormality (low density on CT) indicates a positive node. Shape and an increased number of nodes in a particular region suggest a positive neck. An irregular margin indicating extracapsular spread is an indicator of a positive node. Magnetic resonance imaging, positron emission tomography (PET), ultrasound and many other techniques have been applied to this issue.

Although many imaging strategies are significantly more sensitive than clinical palpation, they are not sensitive enough to confidently predict that the neck is negative and so patients with rN0 necks still are given treatment to the neck. Several clinicians have stated that to withhold treatment would require a test that when negative would be correct 90% of the time. The negative predictive value would be 90% or the false negative rate would be 10%. We are still looking for the ideal test.



Imaging is excellent at determining higher stages of neck positivity. Cutoffs of 3 and 6 cm are easily determined at imaging.

With the advent of combination radiation and chemotherapy for primary and nodal treatment, imaging has taken on a new role. Changes in size at CT and MRI, changes in PET positivity and changes in MRI diffusion have all been applied to follow response. Differences in imaging parameters are used in many institutions to determine if a particular chemotherapy is to be continued. The criteria for neck dissection after partial response to chemotherapy/radiation therapy combinations vary among institutions.

Thyroid carcinoma

The finding of positive nodes in patients with thyroid cancer is less significant than in squamous cell cancer. In papillary ca even small nodes with enhancement, cyst formation or calcification are considered positive on CT. Ultrasound is excellent for characterizing nodes but cannot visualize mediastinal nodes or high retropharyngeal nodes (Rouviere) We do both ultrasound and contrast enhanced CT at the initial diagnosis. Some surgeons prefer classification of nodes as located in the medial and lateral compartments of the lower neck (relative to the carotid artery) or in the upper neck rather than the more elaborate level approach.



Imaging of the Temporal Bones: Key Issues 2011

Hugh D. Curtin MD

*Massachusetts Eye and Ear Infirmary, Harvard Medical School
Boston, MA, USA*

Interpretation of imaging of the temporal bone requires an intimate knowledge of the anatomy. Adopting a standardized image plane simplifies interpretation by allowing the radiologist to more quickly become familiar the complex anatomy. Emphasizing several “index” images provides a solid basis for beginning student.

The anatomy does not change but there have been recent advances in imaging that are applicable to the temporal bone. There have also been advances in clinical approaches to temporal bone disease that have implications in imaging. These advances are most dramatic in the assessment and treatment of conductive hearing loss

As with all imaging the clinical issues must be emphasized. Key landmarks should be assessed for each clinical situation. For instance, in cholesteatoma the standard imaging finding is erosion of the scutum. However the clinician is more interested in the status of the tegmen of the attic and mastoid, the lateral semicircular canal and the facial nerve. Knowledge of the relationship of pathology to these structures is a key part of surgical planning.

The classic description of a cholesteatoma describes erosion of the scutum by a soft tissue mass. However many cholesteatomas will drain spontaneously into the external auditory canal. If there has been bone erosion, the appearance of the defect is very similar to that of a surgical drainage. The surgical removal of a small cholesteatoma may be done through the external canal and is referred to as an atticotomy. The term autoatticotomy has been applied to the appearance of an air filled defect left when a cholesteatoma drains after eroding the scutum and at times the ossicles.

The dehiscence of the superior semicircular canal is a relatively new diagnosis in the field of otology. This is also called the “third window” phenomenon. The defect interferes with the hydraulic integrity of the labyrinth and can result in many different symptoms. The classic symptom is Tullio’s phenomenon. Motion of the labyrinthine fluids allowed by the dehiscence will give dizziness with loud noises. However, the loss of the acoustic energy allowed by the dehiscence also gives a conductive hearing loss. Other symptoms that have been blamed on the dehiscent canal include pulsatile tinnitus and autophony. The higher resolution of new flat panel computed tomography has been applied to this disease.



An approach to evaluation of conductive hearing loss begins with an examination of the tympanic membrane (TM). If there is a white mass or scarring of the TM a cholesteatoma is suspected and erosion of the scutum is sought but the other landmarks that are important issues in surgical planning are emphasized. It should be remembered that acute inflammation can cause resorption of the long process of the incus without cholesteatoma.

If there is a red mass with the conductive hearing loss, the radiologist looks at the carotid plate and the jugular plate to differentiate an aberrant carotid artery from a glomus tympanicum or a glomus jugulare.

If the tympanic membrane is normal with the conductive hearing loss, otosclerosis is a major consideration but a dehiscent superior semicircular canal can present in much the same way. The facial nerve location must be confirmed as the nerve can cross the oval window. If the diagnosis is otosclerosis (look for demineralization just anterior to the stapes in the oval window) make sure that the round window is open.



Post-Treatment Imaging of Head and Neck Cancer

Hugh D. Curtin MD

*Massachusetts Eye and Ear Infirmary, Harvard Medical School
Boston, MA, USA*

There are two major goals of post-treatment imaging of the patients with head and neck cancer. Classically, imaging has been done to search for recurrence or residual tumor. More recently post-treatment imaging has been used to follow and predict response to radiation/chemotherapy protocols.

Recurrence detection

A search for recurrence or residual tumor can use many different tools. There is no universal agreement as to the appropriate protocol. Computed tomography (CT), magnetic resonance imaging (MRI), or positron emission tomography with CT (PET/CT) are the most popular strategies. Obviously, combining PET with CT is a very powerful tool but it is expensive and many begin with a contrast enhanced CT. In tumors of the skull base, sinonasal region, nasopharynx and often the oral cavity/pharynx magnetic resonance is preferred by many radiologists. MRI is considered to be more sensitive for detecting perineural spread and skull base invasion.

If the strategy begins with contrast enhanced CT, the study is scrutinized for areas of soft tissue that cannot be explained as a normal structures or predictable post therapeutic changes. If there are no suspicious areas, the patient is scheduled for the next routine surveillance imaging. Any area that cannot be readily explained is graded and assigned an "index of suspicion." Obvious recurrence or very suspicious areas may undergo biopsy, either direct or using image guidance. Less suspicious areas may be referred to PET/CT. Even less suspicious areas may go to shorter term follow-up imaging. Many radiologists feel comfortable with this strategy but PET/CT is probably ideal if cost were not an issue.

Recently some investigators have emphasized the addition of diffusion weighted magnetic resonance imaging sequences to routine MRI examination. This approach is thought to increase sensitivity and help identify recurrence. In imaging the skull base, there is controversy regarding when to use fat suppression. Some feel that susceptibility artifacts may obscure the nerves within various neural foramina.

In any strategy, knowledge of the therapeutic history is crucial. Ideally the pre therapy images should be available as the location of tumor recurrence or the area most likely to harbor residual disease will be relatively predictable. Knowledge of the different types of resection and flap reconstruction can be very helpful.



With modern chemotherapy/ radiation therapy protocols, imaging has been used to assess response to treatment. Imaging may be used to determine if a particular therapeutic strategy is likely to succeed if continued or if a different strategy should be followed. Many centers use imaging to determine if a neck dissection should be performed after initial therapy or if the neck can be followed with imaging surveillance protocols. There is no universally agreed upon approach. Some recommend neck dissection based on pre-therapeutic imaging. For instance some advise that all patients with imaging evidence of extracapsular spread should undergo neck dissection even if the disease has apparently completely disappeared. Others will follow most necks that appear to be normal after therapy. At least one institution requires that nodes have a PET Standard Uptake Value (SUV) of less than 3 with normal sized nodes before withholding neck dissection. Cystic areas within nodes may push toward dissection as the small solid areas may not give sufficient uptake to be measureable accurately.

In summary, there is no universally agreed upon approach to post therapeutic imaging. There are many tools available. Work to establish the ideal and most effective protocol continues.



The Value of Perfusion Study in Carotid Stenting

Michael Mu Huo Teng

*Department of Radiology, Taipei Veteran General Hospital, Taipei, Taiwan
National Yang Ming University, Taipei, Taiwan*

Outline:

1. Hyperperfusion syndrome after carotid angioplasty and stenting (CAS)
2. Perfusion study can be used for
 - A. Understand the status of cerebral perfusion before and after CAS.
 - B. Predict the possibility of HPS before CAS was performed
 - C. Evaluate if hyperperfusion status is present or not after CAS - can the patient be discharged from the hospital or not.
3. CT perfusion: Technique and pitfall in the performance of CT perfusion, and post-processing
4. MR perfusion

Hyperperfusion syndrome

Hyperperfusion syndrome (HPS): HPS is a clinical presentation that can happen just after the procedures of carotid endarterectomy (CEA) or carotid angioplasty and stenting (CAS) until 4 weeks after procedures (28 days). According to Ogasawara et al, it occurred in 1.4% of all cases of CEA and CAS, 1.9% of cases of CEA, and 1.1% of CAS. The worst clinical presentation is intracerebral hemorrhage (ICH), and occurred in 0.6% in all cases, 0.4% of CEA, and 0.7% of CAS, with mortality of 26% for patients with ICH (Ogasawara K. et al, 2007). Large clinical series about CEA have shown that the overall incidence of ICH complicating the procedure is on the order of 0.2%-0.7%. Hyperperfusion following CEA occurs in some 9-14% of patients, but only a minority develops symptoms (Adhiyaman V et al 2007). For CAS, rates of HPS range from 1.1% to 5% (Meyers, 2000).

Hyperperfusion after operation is classically defined as >100% increase in CBF compared with preoperative values (Sundt TM, 1981). The diagnosis of HPS could be made by postoperative increases in CBF in the ipsilateral hemisphere exceeding the flow in the contralateral hemisphere, as measured using perfusion singlephoton emission CT or cold xenon-enhanced CT, or postoperative increases in middle cerebral artery blood flow velocity of more than 100% of the preoperative values on transcranial Doppler ultrasonography (Ogasawara K. et al, 2007).

Some patients with ICH or clinical HPS did not have typical CBF changes. Although not all ICH after CAS was caused by hyperperfusion syndrome. Other causes of post-CAS ICH could be caused by presence of microaneurysm, hypertension, antiplatelet medication and the use of large dose of heparin at the procedure of CAS. Yet, understanding to HPS, and control of BP in patients with possible hyperperfusion status and those from hypertension would lower the rate of post- CAS ICH.

Generally CAS is a preventive procedure, patients could have no symptoms, or with history of TIA, or minor stroke. Occurrence of sudden ICH with high mortality is not acceptable in such patients with intact neurologically or minor symptoms. Therefore, we have to be ready to prevent the occurrence of hyperperfusion syndrome, and its severe complication of ICH.

Thus understanding HPS itself, the prevention, and management of HPS is of utmost importance for neuroradiologists who perform CAS. Risk factors of HPS includes (Adhiyaman V et al 2007): high grade stenosis w/poor collateral flow; contralateral carotid occlusion; asymmetry index of CBF < 75 %; diminished cerebrovascular reserve; intraoperative ischemia; postoperative hypertension; hyperperfusion lasting more than several hours after CEA.

Predict of HPS can be done by:

1. CT perfusion with Diamox challenge test (Vagal AS, 2009)
2. Elevation of pre-operative CBV (to > 1.38 of contralateral normal side, or > 6.6 ml/100 g) (Fukuda T et al 2007)
3. Low CBF on pre-operative perfusion study (ROI CBF / thalamus CBF < 50% , Normal contralateral <75%): By definition, HPS has a post-operative CBF increased more than twice to that of the pre-operative value. Therefore, if a Diamox challenge test was not performed, we can predict a possibility of HPS after CAS when a pre-operative perfusion study shows low cerebral CBF.

After CAS, before clinical presentation of HPS, we can perform a perfusion study, and calculate the changes in CBF, thus we can decide if a hyperperfusion status is present or not..

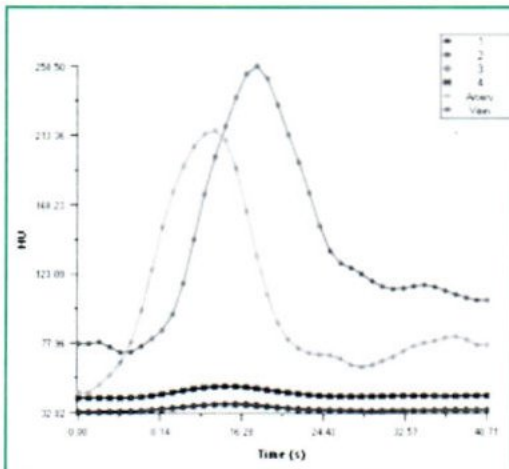
CT perfusion:

Comparing to MR perfusion, CT perfusion has the following advantages:

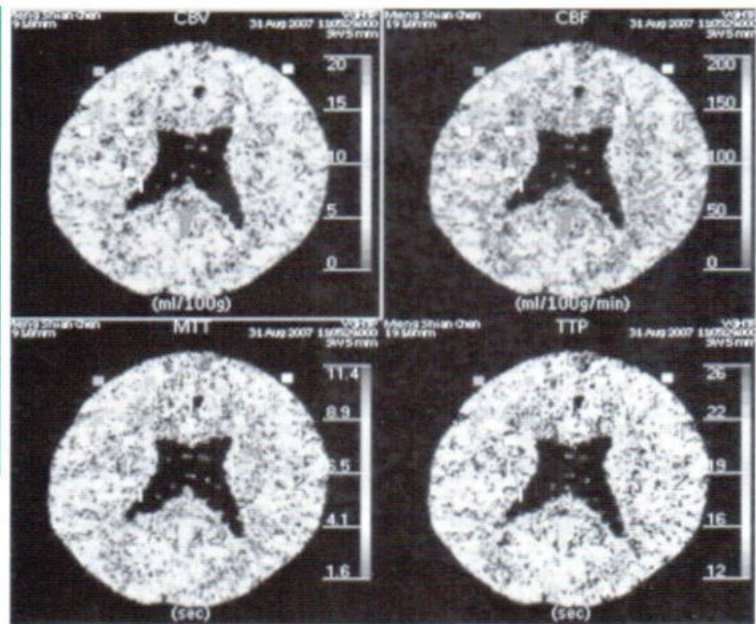
1. Easy to be performed
2. Shorter time needed for postprocessing
3. CSF signal is low and not interfering with information of brain parenchyma.
4. Blood vessels can be removed immediately with current clinical available software.

The disadvantage of CT perfusion is ionizing radiation. We can lower the radiation dose to acceptable value yet keeping a diagnostic quality by adjustment of KVP, MAS, and cycles of the CT perfusion.

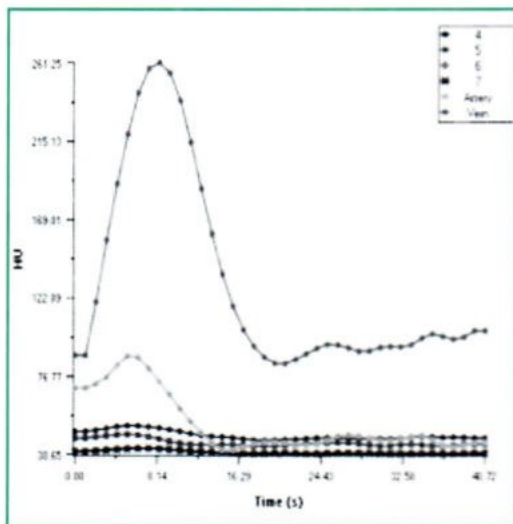
The time of beginning and ending of CT perfusion after injection of contrast media is important in a successful CT perfusion study. A pitfall can occur by poor technique of CT perfusion.



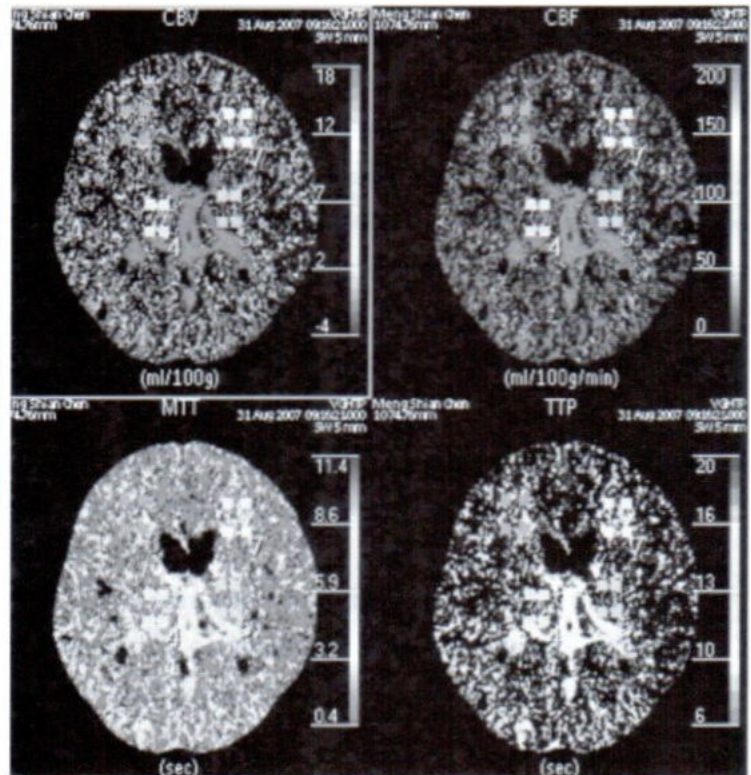
An acceptable concentration-time curve: We have the data before uprising of arterial density, and data of venous density after it returned to the base line.



The data of CT perfusion are acceptable for normal brain: cerebral blood volume (CBV) about 4 ml/100g, cerebral blood flow (CBF) about 5 ml/100 g/min



The concentration-time curve is not acceptable because the data before uprising of arterial curve was not collected, which was caused by long waiting time between injection of contrast media and radiation initiated for data collection

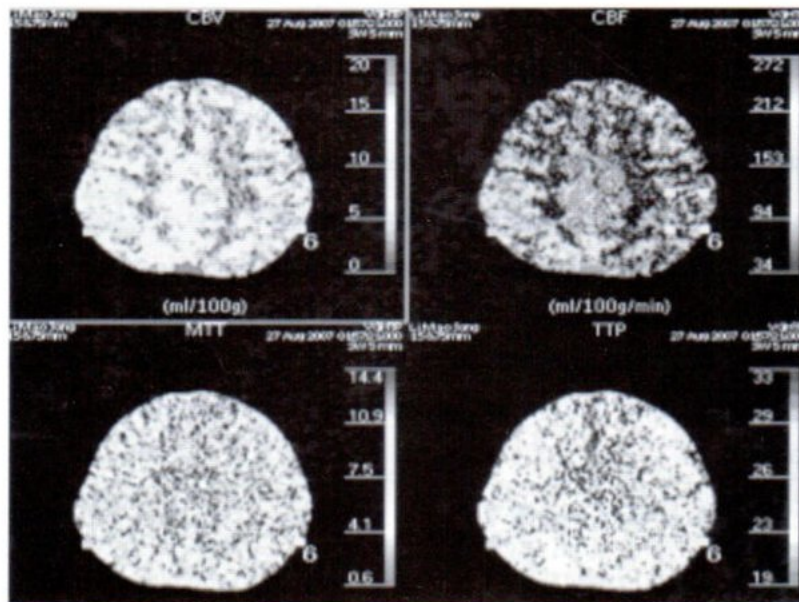


The perfusion data obtained with a wrong concentration-time curve were not acceptable for normal brain: CBV 13 ml/100 g, CBF 187 ml/100 g/min

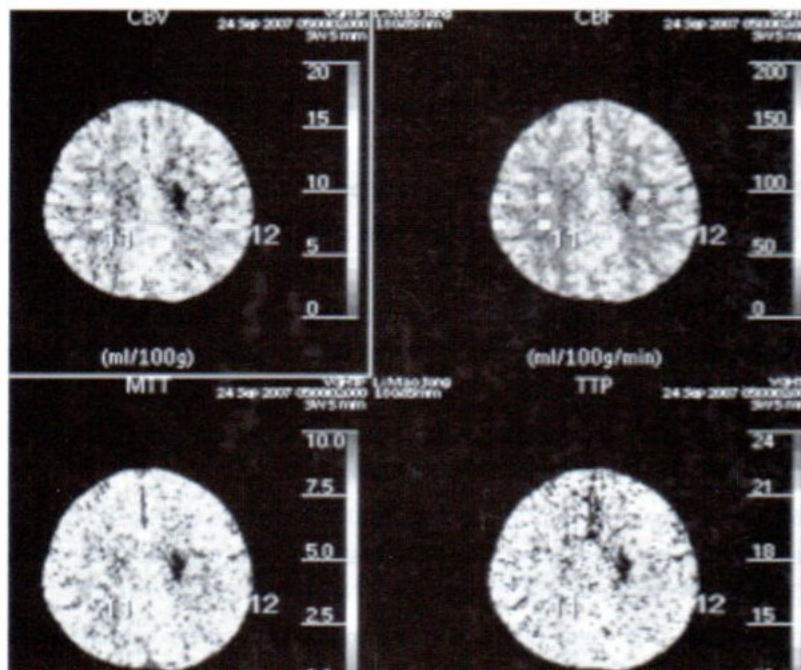
Selecting a proper artery for arterial input function is important, because selecting different artery may have different result.

CT perfusion performed prior to angioplasty and stenting of carotid artery can be used to predict if hyperperfusion is a risk of the patient after carotid stenting. CTP performed after stenting can demonstrate if hyperperfusion state is present or not.

Below is an example of CT perfusion demonstrating hyperperfusion syndrome:



The CT perfusion shows increased CBF, CBV and shortening of MTT in right parietal region, compatible with HPS. The patient had post-CAS seizure, temporal contralateral hemiparesis.



Follow up CT perfusion 1.5 months later after resolution of clinical symptoms. The perfusion is now normal and symmetrical.



MR perfusion:

Dynamic susceptibility contrast-enhanced MR perfusion from current MR scanner does not provide absolute data of CBF, CBV, and MTT. Different MR scanner provides different methods of calculation. In addition, CSF was not removed, and CSF signal could be similar to the normal or abnormal brain, thus interfere with the clinical judgment of brain perfusion.

The technique of CSF removal has reported recently (Kao YH et al). The reason of not providing absolute data from MR perfusion obtained from a clinical MR scanner is caused by the unreliability of venous of output (VOF) function because of artifact in a big vein, and the non-linearity between the signal and density of contrast in the vein in MR perfusion. Some research softwares for post-processing of MR perfusion do provide absolute data. After testing with our cases, we found that many of these data obtained with these softwares are not acceptable, because of too high or too low in the normal brain.

There are different convolutional methods for post-processing of MR perfusion. CBF and MTT obtained with standard singular value deconvolution (sSVD) provide the best contrast between the normal and abnormal brain with a high sensitivity in the detection of the lesion with low perfusion. MTT and CBF calculated with circulant singular value deconvolution (cSVD) is less sensitive in detecting the lesion. cMTTc is least sensitive in detecting lesion side thus is not acceptable for clinical use. The cMTTc is obtained by the following calculation:

$$\text{cMTTc} = \text{CBV} / \text{cCBF}$$

where cCBF was calculated with cSVD.

References

1. Ogasawara K, Sakai N, Kuroiwa T, et al. Intracranial hemorrhage associated with cerebral hyperperfusion syndrome following carotid endarterectomy and carotid artery stenting: retrospective review of 4494 patients. *J Neurosurg* 2007;107:1130-6.
2. Adhiyaman V, Alexander S. Cerebral hyperperfusion syndrome following carotid endarterectomy. *QJM* 2007;100:239-44.
3. Meyers PM, Higashida RT, Phatouros CC, et al. Cerebral hyperperfusion syndrome after percutaneous transluminal stenting of the craniocervical arteries. *Neurosurgery* 2000;47:335-43.
4. Sundt TM Jr, Sharbrough FW, Piepgras DG, Kearns TP, Messick Jr, O'Fallon WM. Correlation of cerebral blood flow and electroencephalographic changes during carotid endarterectomy: with results of surgery and hemodynamics of cerebral ischaemia. *Mayo Clin Proc* 1981;56:533-43.
5. Vagal AS, Leach JL, Fernandez-Ulloa M, Zuccarello M. The Acetazolamide Challenge: Techniques and Applications in the Evaluation of Chronic Cerebral Ischemia. *AJNR Am J Neuroradiol* 2009;30:876-84.
6. Fukuda T, Ogasawara K, Kobayashi M, Komoribayashi N, Endo H, Inoue T, Kuzu Y, Nishimoto H, Terasaki K, Ogawa A. Prediction of Cerebral Hyperperfusion after Carotid Endarterectomy Using Cerebral Blood Volume Measured by Perfusion-Weighted MR Imaging Compared with Single-Photon Emission CT. *AJNR Am J Neuroradiol* 2007;28:737-42.
7. Kao YH, Teng MMH*, Zhang WY, Chang FC, Chen YF. Removal of CSF pixels on brain MR perfusion images using first several images and Otsu's thresholding technique. *Magnetic Resonance in Medicine* 2010;64:743-8.



Nasopharyngeal Carcinoma

Vincent Chong

Department of Diagnostic Radiology, Yong Loo Lin School of Medicine, National University of Singapore

Nasopharyngeal carcinoma (NPC) is a unique malignancy, representing the outcome of interactions of genetic factors, environmental factors and the Epstein-Barr virus (EBV). Patients with NPC show consistently high levels of antibodies to EBV antigens and these antibodies are very useful diagnostic markers. NPC also shows a unique geographical distribution. The highest incidence rates (up to 50 per 100,000 population) are found in Southern China, Hong Kong and Chinese elsewhere in Southeast Asia.

Radiation therapy is the mainstay of treatment. NPC is distinct from the other squamous cell tumors of the head and neck. It shows aggressive local infiltration and a high frequency of cervical nodal metastasis despite apparently early primary lesions. Systemic failure is also common in patients with locally advanced disease. Chemotherapy is usually used for recurrent or metastatic disease but in recent years, a combination of radiation and chemotherapy has been tried for treatment of locally advanced disease. Surgery plays only a minor role and is limited to resection of residual or recurrent disease in the nasopharynx and neck nodes.

Pathologic Anatomy

Most tumors originate in the fossa of Rosenmuller and spread along well-defined routes.

Anterior spread

Tumors often spread anteriorly into the nasal fossa and may infiltrate the pterygopalatine fossa (PPF) through the sphenopalatine foramen. Once the tumor gains access into the PPF, tumor can extend along the maxillary nerve and through the foramen rotundum into the cranium. Tumor in the PPF may spread further superiorly into the inferior orbital fissure and the orbital apex. From the orbital apex tumor can readily extend intracranially through the superior orbital fissure.

Lateral spread

This is the most common direction of spread and can be recognized by infiltration of the fat-filled parapharyngeal space (PPS). Further lateral spread involves the masticator space (MS). Once the tumor involves the PPS or MS the mandibular nerve is vulnerable to perineural infiltration and subsequent intracranial extension.

Posterior spread

NPC can extend posteriorly infiltrating the retropharyngeal space (RPS) and prevertebral muscles. Posterolateral spread results in the encasement or infiltration of the carotid sheath. Posteroinferior extension may involve



jugular foramen and the adjacent hypoglossal canal thus endangering the last four cranial nerves. Subsequent spread into the posterior cranial fossa is not uncommon.

Inferior Spread

Some tumors show preferential inferior spread along the pharyngeal wall. This may take place submucosally and thus escapes endoscopic detection. Submucosal spread into the oropharynx can readily be detected on imaging studies. The oropharyngeal wall shows subtle to gross wall thickening. Tumor may also spread along the retropharyngeal space. Hence, imaging plays an important role in accurate tumor staging and mapping. However, in advanced cases, the tumor in the oropharynx may be clearly seen during clinical examination.

Superior Spread

When NPC spreads superiorly it may erode the clivus, sphenoid sinus floor, petrous apex, and the foramen lacerum. Skull base erosion is detected in up to one-third of the patients. For a long time, NPC was believed to spread intracranially mainly through the foramen lacerum. However, on MRI the most common route involves the foramen ovale.

Metastasis

Cervical nodal metastasis is common in NPC. Often, it is the enlarged neck nodes that prompt initial medical consultation. Seventy-five percent of patients have enlarged cervical nodes at presentation. Nodal metastasis show an orderly inferior spread and the affected nodes are larger in the upper neck.

NPC shows a high frequency of distant metastasis compared with other tumors of the head and neck. Patients with low cervical lymphadenopathy, especially in the supraclavicular fossa, have a significantly higher risk of distant metastasis. This observation can be explained by the nature of the lymphatic drainage of the head and neck. Lymph flows down the neck and the supraclavicular nodes form the last defensive barrier to the spread of malignant cells within the lymphatic vessels. Malignant cells upon escaping the supraclavicular nodes enter the thoracic duct and subclavian vein resulting in systemic dissemination. Alternatively, tumor cells upon spreading into the PPS enter the parapharyngeal venous plexus resulting in systemic spread.

Tips, Tricks and Pitfalls of Clinical DTI

Kei Yamada M.D., Ph.D.

Department of Radiology, Graduate School of Medical Science, Kyoto Prefectural University of Medicine

Kajii-cyo, Kawaramachi Hirokoji Sagaru, Kamigyo-ku, Kyoto City, Kyoto 602-8566, Japan

Diffusion-tensor imaging (DTI) has now become one of the essential research/clinical tools in analyzing the brain in both normal and pathological states. Water diffusion preferentially diffuses in a direction parallel to the axon's longitudinal axis but is relatively restricted in the perpendicular axis. This phenomenon can be represented mathematically by the so called diffusion ellipsoid, or tensor. The diffusivity along the principal axis, λ_1 is also called the longitudinal, axial, or parallel diffusivity.

The tensors of cerebral white matter can be reconstructed to track three-dimensional macroscopic fiber orientation in the brain. The translation of the longest axis of the tensor (v_1) into neural trajectories can be achieved by various algorithms, among which the FACT algorithm will be one of the most frequently used[1]. The tractography technique allows *in vivo* localization of neuronal fiber tracts, which was not previously possible. As a clinical tool, this technique primarily targets the intracranial space occupying lesions, i.e. brain tumors and vascular malformations[2-3]. This has been also utilized for other conditions, such as stroke imaging [4-6] and in assessing degenerative diseases[7-12].

It is important to notice that DTI is prone to partial volume averaging especially at the areas with crossing fibers[12]. Thus, when comparing results from different institutes, it will be ideal to standardize the voxel size to avoid this effect. The most important limitation of tractography will be that it has not yet been fully validated. Attempts to validate this technique have been made in the past[13,14], but are limited to comparisons of the tractographic images and known neuroanatomy. One has to interpret the results with cautions when applying this technique clinically[15].

References

1. Mori S, et al. Three-dimensional tracking of axonal projections in the brain by magnetic resonance imaging. *Ann Neurol* 1999;45:265-9.
2. Nimsy C, et al. Intraoperative visualization of the pyramidal tract by diffusion-tensor-imaging-based fiber tracking. *Neuroimage*. 2006;30:1219-29.
3. Yamada K, et al. Clinically feasible diffusion-tensor imaging for fiber tracking. *Radiology* 2003;227:295-301.
4. Kunitatsu A, et al. Three dimensional white matter tractography by diffusion tensor imaging in ischaemic stroke involving the corticospinal tract. *Neuroradiology* 2003;45:532-5.



5. Konishi J, et al. MR tractography for the evaluation of the functional recovery from lenticulostriate infarct. *Neurology* 2005; 64:108-13.
6. Sakai K, et al. Diffusion tensor imaging may help the determination of time at onset in cerebral ischaemia. *J Neurol Neurosurg Psychiatry* 2009;80:986-90.
7. Taoka T, et al. Fractional anisotropy--threshold dependence in tract-based diffusion tensor analysis: evaluation of the uncinate fasciculus in Alzheimer disease. *AJNR Am J Neuroradiol* 2009;30:1700-03.
8. Yoshiura T, et al. Mapping of subcortical white matter abnormality in Alzheimer's disease using diffusion-weighted magnetic resonance imaging. *Acad Radiol* 2006;13:1460-4.
9. Aoki S, et al. Quantitative evaluation of the pyramidal tract segmented by diffusion tensor tractography: feasibility study in patients with amyotrophic lateral sclerosis. *Radiat Med* 2005;23:195-9.
10. Provenzale JM, et al. Quantitative analysis of diffusion tensor imaging data in serial assessment of Krabbe disease. *Ann N Y Acad Sci* 2005;1064:220-9.
11. Filippi M, et al. Diffusion tensor magnetic resonance imaging in multiple sclerosis. *Neurology* 2001;56:304-11.
12. Oouchi H, et al. Diffusion anisotropy measurement of brain white matter is affected by voxel size. *AJNR Am J Neuroradiol* 2007;28:1102-6.
13. Okada T, et al. Corticospinal tract localization: integration of diffusion-tensor tractography at 3-T MR imaging with intraoperative white matter stimulation mapping. *Radiology* 2006;240:849-57.
14. Kinoshita M, et al. Fiber-tracking does not accurately estimate size of fiber bundle in pathological condition. *Neuroimage* 2005;25:424-9.
15. Yamada K. Diffusion tensor tractography should be used with caution. *Proc Natl Acad Sci U S A*. 2009 106:E14

Clinical Applications of CT Perfusion in Neuroimaging

Kazuhiro Katada, Japan

CT perfusion (CTP) has gained widespread acceptance as a noninvasive method for assessing cerebral blood flow. However, in conventional CTP, only a limited range of the brain can be scanned due to the limited detector width. The introduction of 320-row area detector CT, which can cover a wide range of 160 mm in a single rotation, has made it possible to perform CTP for the entire brain. This whole-brain CTP method has the following advantages: 1) the entire brain can be scanned, eliminating the possibility of missing a lesion in the parietal region or posterior cranial fossa, 2) remote effects such as crossed cerebellar diaschisis can be assessed, 3) whole-brain 4D-CT angiographic images can also be generated from the time-sequential dataset acquired for CTP, and 4) all required CT data can be obtained by executing a single scan sequence, reducing the amount of contrast medium used and minimizing patient discomfort.

In clinical examinations performed at our institution for patients with early ischemic cerebrovascular disease, the findings of whole-brain CTP showed good agreement with those of conventional SPECT. For patients with hyperacute ischemic cerebrovascular disease within 6 hours after onset, the area of reduced cerebral blood flow observed in CTP images showed good agreement with the area seen in MR diffusion-weighted images (DWI), as reported in previous studies. In addition, the area in which the mean transit time (MTT) or time to peak (TTP) was prolonged showed good agreement with the definitively identified infarcted region. Whole-brain CTP, which permits both CTP data to be obtained and the morphological characteristics of the cerebral blood vessels and blood flow direction to be evaluated by executing a single scan sequence within 1 minute, is therefore considered to be very useful for the evaluation of patients with hyperacute ischemic cerebrovascular disease, in whom rapid diagnosis and immediate treatment are essential. This method, which permits both the morphological characteristics of the cerebral blood vessels and hemodynamics to be examined simultaneously, is also suitable for assessing patients before and after superficial temporal artery to middle cerebral artery anastomosis as well as for evaluating cerebrovascular contraction after cerebral aneurysm surgery.

The main limitation of this method, in which the same region is scanned repeatedly more than ten times, is the increased exposure dose. However, the recently introduced iterative reconstruction method makes it possible to acquire highly reliable CTP data with a low exposure dose. Area detector CT, which permits the entire brain to be scanned in a single rotation, is expected to play a major role in the diagnosis of various intracranial diseases such as ischemic cerebrovascular disease.



Imaging of Orbital Neoplasms

Sukalaya Lerdlum, MD *

Tumor and tumorlike lesions of the globe, optic nerve sheath complex, nonosseous and osseous extraocular orbit in children represents a different histologic spectrum than in adults. Most primary and metastatic ocular neoplasms in adult involve the uveal tract and in particular the choroid. Malignant melanoma is the most common tumor to involve the uvea. Uveal metastasis can be confused clinically and radiologically with uveal melanoma. The most common sources of secondary tumor within the eye are the breast and lung. Most common primary ocular neoplasms in children, however, involve the retina. Retinoblastoma is a tumor of infancy and the most common intraocular tumor in children. The most common clinical finding is leukocoria. The differential diagnosis of this sign include several nonneoplastic lesions.

Optic nerve sheath complex lesions encompass a wide spectrum of different disease entities, including inflammatory disease, benign tumors, primary and secondary malignant tumors, and miscellaneous abnormalities. The most common primary optic nerve tumor is the optic nerve glioma, followed by the optic nerve meningioma. Optic nerve glioma is the most common tumor of the the optic nerve in children and is frequently associated with neurofibromatosis type I. Optic nerve sheath meningiomas, shown by symmetric or asymmetric thickening of the nerve, occur most commonly in middle-aged women and display slow growth with gradual progressive deterioration in vision.

Rhabdomyosarcoma is the most common malignant extraocular tumor in children. This neoplasm usually manifests in young children, grows quite rapidly. Vasculogenic lesions are common orbital lesions in newborn and young infants. The most prevalent of these are infantile hemangioma. All of extraocular masses typically manifest with proptosis.

Some primary bone lesions may involve the orbit, producing a lytic or dense lesion with enlargement of the bone; these lesions include fibrous dysplasia, juvenile ossifying fibroma and osteosarcoma. Langerhans cell histiocytosis, an idiopathic reticuloendothelial proliferative disorder, tends to involve the bones of skull including the orbit. The orbit is also a common site of bone metastases from neuroblastoma in young children.

In the lacrimal gland, about half of the mass are epithelial neoplasms, and the other half are caused by lymphoproliferative or inflammatory disorders. Pleomorphic adenoma occurs for half of the epithelial neoplasm of lacrimal gland with slow growing features. Adenoid cystic carcinoma is the most common malignant epithelial tumor of lacrimal gland. Other malignant tumors of lacrimal gland include mucoepidermoid



carcinoma, anaplastic carcinoma, and primary adenocarcinoma. Lymphoma and other lymphoid tumors of lacrimal gland are secondary involvement from extraorbital origin.

Knowledge of the pathological features of these orbital tumors and how these features are reflected in their imaging appearances may help radiologists differentiate them.



Imaging of Inflammatory and Demyelinating Disease of Spinal Cord in Asian Patients

Orasa Chawalparit, MD., Naraporn Prayoonwiwat, MD.

*Department of Radiology, Department of Medicine, Faculty of Medicine Siriraj Hospital,
Mahidol University, Bangkok, Thailand*

Myelopathy is clinically defined as a neurological process to spinal cord. Acute myelopathy is distinguished from mimics on clinical ground. Transverse myelitis is a syndrome of myelopathy defined as an interruption in ascending and descending neuroanatomical pathway in the transverse plane of spinal cord and a resulting sensory level. Half of the cases could not be diagnosed initially with certainty and 15-30% were finally classified as idiopathic cause. Differential diagnosis can be made by combining clinical course and characteristic high T2 lesion in the spinal cord on MRI. Most of the literatures suggested MRI with gadolinium enhanced imaging as a first investigation when approaching patients with acute myelopathy in order to rule out compressive cord and infective myelitis. If intramedullary cord is absent, reconsidering myelopathy diagnosis is suggested. When abnormal enhancement on MRI, CSF analysis and IgG are found, diagnosis mostly fall into the group of infection, autoimmune disease and malignancy. Patterns of myelitis are helpful for cases with negative findings.

After excluding neoplasm and syringomyelia, the etiologic classification of myelitis could be idiopathic transverse myelitis, inflammation and autoimmune/demyelinating disease, infection, metabolic cause, vascular cause and toxic myelitis.

Multiple sclerosis and Neuromyelitis Optica

In Asia-Pacific countries, 3 major characteristics of patients with multiple sclerosis (MS) and neuromyelitis optica (NMO) were different from Western countries. The first is lower prevalence of MS in Asian (less than 5/100,000 in most Asia, 8-10/100,000 in Japan VS 30-200/100,000 in Western). The second is higher ratio of NMO to MS in Asian than in Western (1:2 to 1:10 VS 1:1,000 respectively). The last one is more atypical MS in Asian. Many studies from Western patients were concluded to set the diagnostic criteria to differentiate between MS and NMO. The most popular ones are McDonald's criteria for MS and Wingerchuck's criteria for NMO.

Aquaporin (AQP) is a water channel receptor regulating water homeostasis. There is a subtype of AQP4 receptor was found in CNS tissue. The antibody (Ab) to AQP4 receptors was found in serum of many

autoimmune disease including NMO, SLE and Sjogren disease. NMO IgG was reported to be the same as anti-AQP4 Ab. The AQP4 receptor was found mostly along the ependymal layer of lateral ventricle, third/fourth ventricle, area postrema, basal ganglion and hypothalamus. Patients with positive Ab but not fulfilled NMO criteria were classified as NMO spectral disorder (NMOSD). Abnormal lesions on brain MRI were found in the common locations with AQP4 in these patients in most studies.

Many reports from Asian countries including Thai found different imaging characteristics in NMO comparing with Western cases. Siritho S, et al reported positive AQP4 Ab in 39.3% of 135 cases with idiopathic inflammatory demyelinating disease. When classified all the 135 cases with clinical and MRI criteria of Western reports, positive Ab was found in 78% of NMO, 44% of NMOSD, 57% of opticospinal MS, 24% of classic MS, and 6.3% of clinical isolated syndrome. Chawalparit O, et al reported long extensive spinal cord lesion (LESL \geq 3 vertebral body segment) in 66.7% of 33 positive Ab patients. They also found significant difference of MRI findings in patients with Ab positive and negative. The LESL and central cord location on axial plane were found more in antibody positive group, whereas peripheral cord location and swelling were found more in antibody negative cases. On brain MRI, lesions along the subependymal third/fourth ventricle was also reported more in Ab positive group. Surprisingly, there was no difference of cases fulfilled Barkhof's criteria between both groups.

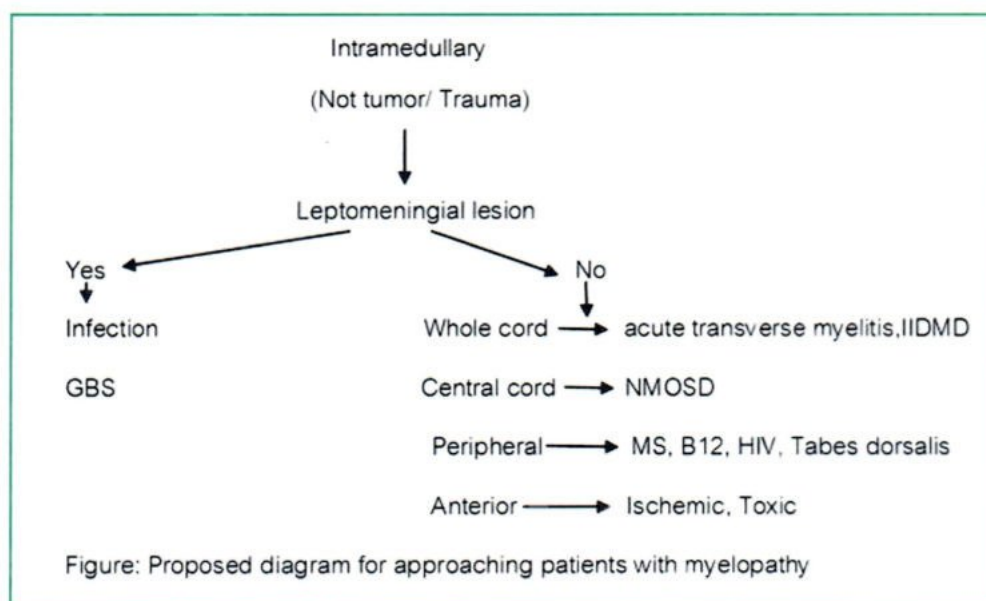
From all of these evidences, many experts opinion concluded different clinical and MRI characteristics of MS and NMO in the Asian from Western countries. Characteristics of lesion and location are more important for diagnosis in Asian patients, not the number of the lesions as in the Western patients. Analysis of AQP4 Ab is also essential for Asian cases.

Differential Diagnosis of demyelinating disease of spinal cord

1. Infection: viral, bacteria, tuberculosis, syphilis
2. Parasitic infestation: gnathostomiasis, angiostrongyliasis, cysticercosis
3. HIV myelitis, vacuolar myelopathy
4. B12 deficiency
5. Spinal dural AVM
6. Ischemic and toxic substance

The most common cause of myelitis in Asian countries is still falling into infection, especially parasitic infestation. Gnathostomiasis and angiostrongyliasis are common causes of eosinophilic myelitis in Northeast Thailand. Through cysticercosis is not commonly involved spinal cord, in certain severe cases, cord lesion could be found.

Other rare causes including B12 deficiency, spinal dural AVM, and back coming tabes dorsalis should be considered. The following diagram is proposed for MRI analysis of patients with myelopathy and myelitis.



In conclusion, spinal MRI is the investigation of choice for approaching patients with acute myelopathy. When demyelinating disease is suspected, brain MRI should be performed. Characteristic location rather than the number of the lesions should be considered for Asian MS and NMO.

References

- Schmalstieg WF, Weinshenker BG. Neurology(r) Clinical Practice 2010;75(Suppl 1):S2-S8.
- Bou-Haidar P, Peduto AJ, Karunaratne N. Journal of Medical Imaging and Radiation Oncology 53 (2009) 152-19.
- Frohmman EM, Wingerchuk DM. N Engl J Med 2010;363:564-72.
- Sheerin F, Collison K, Quaghebeur G. Clinical Radiology (2009) 64, 84e94
- Bassi SS, Bulundwe KK, Greeff GP, Labuscagne JH, Gledhill RF. Neuroradiology (1999)41:271-4.
- Sellner J, Boggild M, Clanet M, Hintzen RQ, Illes Z, Montalban X, et al. European Journal of Neurology 2010;17:1019-32.
- Kim W, et al. Multiple sclerosis 2010;16(10):1229-36.
- Matsushita T, et al. Multiple sclerosis 2009;15:834-7.
- Matsushita T, et al. J Neurol Sci 2010;291:37-43.
- Matsushita T, et al. Brain 2007;130:1206-23.
- Barkhof F, et al. Brain 1997;120:2059-69.
- McDonald WI, et al. Ann Neurol 2001;50:121-7.
- Takahashi T, et al. Brain 2007;130:1235-43.
- Siritho et al. Neurology August 2011;77
- Chawalparit O, Peanpat W, Jitpratoom P, Siritho S, Prayoonwivat N. PACTRIM2011.
- Sawanyawisuth K, Tiamkao S, Kanpittaya J, Dekumyoy P, Jitpimolmard S. AJNR Am J Neuroradiol 2004;25:446-9.
- Schmutzhard E, Boongird P, Vejajiva A. J Neurol, Neurosurg, Psychiat 1988;51:80-7.
- Prabhakar S, Syal P, Singh P, Lal V, Khandelwal N, Das CP. Neurol India 1999;47:294.

Spinal Infection

Jureerat Thammaroj

Department of Radiology, Faculty of Medicine, Khon Kaen University

Spinal infections are rare. The incidence of acute hematogenous nontuberculous vertebral osteomyelitis is estimated to be 5-5.3 patients per million patients per year with a male predominance¹⁻³. The axial skeleton accounts for 2-7% of all patients with osteomyelitis³⁻⁵. An increase in vertebral osteomyelitis has been noted during the last 15 years, probably as a result of the evolutions in diagnostics^{2,5}.

Spinal infection in adults may affect the vertebral bodies, the intervertebral disks, the spinal canal, and the paravertebral tissues and structures; hence, their categorization as vertebral osteomyelitis, spondylodiskitis, epidural abscess, and paravertebral infection. Spinal infections pose a unique diagnostic problem, as they affect a wide range of patients and may run a subtle clinical course.

Magnetic resonance imaging is currently a modality of choice for the evaluation of a potential spinal infection⁶⁻¹⁰. Advantages of MR imaging include the capacity of multiplanar imaging, direct evaluation of the affected spinal cord, bone marrow and contemporary visualization of the neural structures¹¹.

Spinal tuberculosis is the most common site of osseous involvement in tuberculosis. The disease prevalence will continue to rise as the number of immunocompromised patients increases. On our review, In North Eastern part of Thailand we found increasing prevalence of atypical pattern of tuberculosis and the most common pattern is contiguous plus skip pattern. Neurological complications occur in about 10% of patients and can be devastating. Paraplegia may be a result of spinal cord compression from compromising to spinal cord artery either or from liquid or caseous pus, inflammatory granulation tissue of active disease. To prevent the neurological complication, MRI features which may sometimes help to discriminated between type of infections such as pyogenic or tuberculosis should be recognized. MRI features may help to decided antibiotic treatment and necessary for avoiding this long-term disability.

References

1. Tsiodras S, Falagas M. Clinical assessment and medical treatment of spine infections. Clin Orthop 2006;444:38-50.
2. Jaramillo-de Torre JJ, Bohinski RJ, Kungtz C IV. Vertebral osteomyelitis. Neurosurg Clin N Am 2006;17:339-51.
3. Butler JS, Shelly MJ, Timl; in M, et al. Nontuberculous pyogenic spinal infectiojn in adults. A 12-year experience from a tertiary referral center. Spine 2006;31:2695-700.
4. Grammatico L, Besnier JM. Spondylodiscites infectieuses. Rev Prat 2007;57:1-9.
5. Govender S. Spinal infections. J Bone Joint Surg [Br] 2005;87-B:1454-8.



6. Turunc T, Demiroglu YZ, Uncu H, et al. A comparative analysis of tuberculous, brucellar and pyogenic spontaneous spondylodiscitis patients. *J Infect* 2007;55:158-63.
7. Luk KD. Spinal tuberculosis. *Curr Opin Orthop* 2000;11:196-201.
8. Modic MT, Feiglin DH, Piraino DW, Boumphrey F, Weinstein MA, Duchesneau PM, et al. Vertebral osteomyelitis: assessment using MR. *Radiology* 1985;157-66.
9. Post MJ, Quencer RM, Montalvo BM, Katz BH, Eismont FJ, Green BA. Spinal infection: evaluation with MR imaging and intraoperative US. *Radiology* 1988;169:765-71.
10. Sharif HS. Role of MR imaging in the management of spinal infections. *AJR Am J Roentgenol* 1992;158:1333-45.
11. Thrush A, Enzmann D. MR imaging of infectious spondylitis. *AJNR Am J Neuroradiol* 1990;11:1171-80.

Imaging of the Postoperative Spines and Failed Back Syndrome

Jiraporn Laothamatas, M.D.

Spines have two main functions; one is to protect the neural elements, spinal cord and nerve roots, and two to keep human in the upright position. Anything causes failure in these tasks will need to be corrected. There is surgical treatment to remove compressive lesion upon the neural elements such as spinal stenosis, nerve root compression, spinal cord compression, etc. and surgery to correct the alignment and height of the vertebrae to keep the physiologic upright of the human posture. There are several surgical procedures such as open surgery and minimal invasive procedures with or without fixing devices. To be able to interpret the post operative imaging correctly, knowledge of how the procedures have been done and what kind of device has been used are crucial. The preoperative images are also important for comparison with the postoperative images for evaluation of the post operative insult.

Post operative complications can be early or late complications and can be classified into the post-surgical group and post-minimal invasive procedure group. For the early complications, it can be post operative hemorrhage, superimposed infection, pseudomeningocele due to dural tear, residual/recurrent disc herniation or migration of the fixing device. For the late complications, recurrent disk herniation, post operative granulation encasing the nerve roots or thecal sac causing thecal sac stenosis, spinal instability, radiculitis and arachnoiditis are possible. Or infrequently, a foreign body granulation due to left over surgical materials is also found.

In case of instrumentation, prosthesis or cage placement, to evaluate for the proper position or migration of these devices is crucial. To evaluate for instrument failure by searching for evidence of solid bony fusion is also crucial. CT is better than MRI in evaluating details of solid bony fusion. Type of instrumentation and surgical approach as well as expected result is a fundamental knowledge that the radiologist should understand before interpreting the study of post instrumentation evaluation.

Imaging modalities in evaluating postoperative spines are composed of plain films, myelography, CT and MRI and rarely SPECT. Plain film is used mainly to assess the fixing device such as screws, rods and cages. Dynamic plain films are also used to assess the spinal stability. CT is good in evaluating the detailed bony structure such laminotomy or laminectomy defect, bone graft, pseudoarthrosis. It is good in evaluating lateral recess stenosis and central spinal canal stenosis due to bony elements. It is also good in checking the position of the implanted device such as bone plug or metallic device. MRI is considered to be the



modality of choice in evaluating the postoperative spines due to its excellent in differentiating the soft tissue details for both surgical and minimal invasive procedures. It is sensitive in differentiating recurrent disc herniation from postoperative granulation tissue. It also is sensitive in assessing the age of vertebral compression fracture by the bone marrow signal intensity related to surgical or intervention procedure. Nerve root enhancement due to radiculitis or clumping and adhesion of the roots related to the thecal sac in arachnoiditis are better and more accurately detected by MRI compared to CT scan. This also hold true in evaluating the postoperative diskitis and osteomyelitis. SPECT nuclear medicine using thallium is used in the case that infection is suspected and cannot be certainly answer by MRI.

References

1. Sanders WP, Truumees E. Imaging of the postoperative spine. *Semin Ultrasound CT MR* 2004;25:523-35.
2. Van Goethem JW, Parizel P., Jinkins R: Review article: MRI of the post-operative lumbar spine. *Neuroradiology* 2002;44: 723-39.
3. Jinkins R., Van Goetern JW. The post-surgical lumbosacral spine. MRI evaluation following intervertebral disk surgery, surgical decompression, intervertebral bony fusion and spinal instrumentation. *Radiol Clin North Am* 2001;39:1-29.
4. White LM, Buckwalter KA. Technical considerations: CT and MR imaging in the postoperative orthopedic patient. *Semin Musculoskelet Radiol* 2002;6:5-17.
5. Rutherford EE, Tarplett LJ, Davies EM., Harley JM, King LJ. Lumbar Spine Fusion and Stabilization: Hardware, Techniques, and Imaging Appearances. *RadioGraphics* 2007;27:1737-49.

Update in Aneurysm Treatment

IN SUP CHOI, M.D.

Director, Interventional Neuroradiology, Lahey Clinic Medical Center

Professor of Radiology, Tufts University, School of Medicine

Background

Development of detachable coil system by Guido Guglielmi in 1990 revolutionized management of intracranial aneurysms. Clinical trial of GDC proved safe and effective even in treating surgically difficult aneurysms, therefore, it was approved by the Food Drug Administration of U.S. government in 1995.

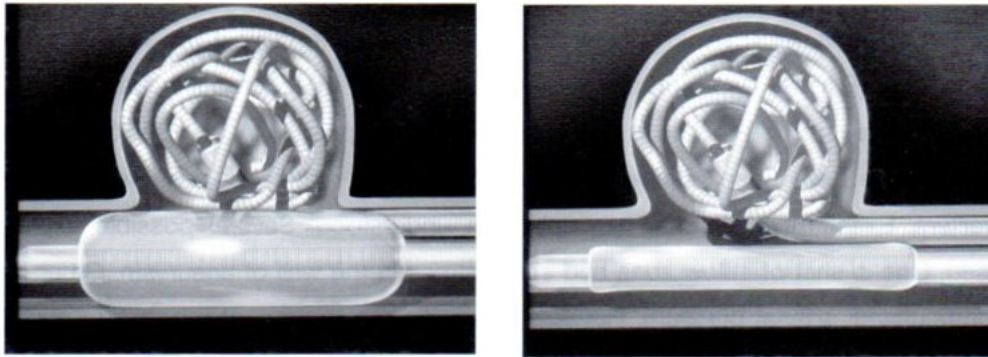
GDC system : Clinical experiences taught us it is necessary to form proper baskets of coils fit to contour of aneurysm wall and subsequent tight filling of rest of the space to achieve more permanent and complete occlusion. It is calculated the volume of coils in relation to volume of aneurysm reaches only up to 28 % on basis of in vitro and in vivo studies in animals. In cases, aneurysm lumen are not tightly packed, recanalization has been observed. Constant hemodynamic stress on a coil mesh causes fatigue of coil loops inducing coil compaction, then, recanalization of aneurysm. The latter mechanism is more obvious in bifurcation aneurysms such as aneurysms in the top of basilar artery, internal carotid bifurcation or anterior communicating arteries. Another factor is presence of thrombus in the aneurysm lumen. Partially thrombosed aneurysms exerts high incidence of recanalization following coil treatment. Even in experienced hands, recanalization in a year follow up have been reported up to 30 % in those special circumstances.

New generation of coils : Research and investigation have continued to improve long term results of endovascular treatment. Newer designs and materials have been tested and now several new coil systems are available. Complex shaped or 3-D coils make relatively easy to fit first coils into the contour of lumen of aneurysm and provide a more stable frame and consequently reduce a chance of coil compaction. Other innovation was development of coated coils. One of those is bioactive coils, Matrix coils. Platinum coils are coated with copolymer, polyglycolic/ polyactic acid (PGA/PLA). It is reabsorbable bioactive material which induces production of mature connective tissue in aneurysm lumen. More aneurysm lumen is filled with mature organized fibrotic tissue, is less chance of recanalization. Other coil system is Hydrocoils. Similar to Matrix coils, platinum coil is covered with hydrogel. This hydrogel swells 3 times of original thickness when contacted with blood. Once placed in the aneurysm lumen, it expands filling more volume of aneurysm, therefore, improve healing at the neck. Thick neointima growth has been shown in animal studies. Clinical investigations revealed somewhat less recanalization rate.



Wide Neck Aneurysm treatment : Wide neck is defined as the face of aneurysm is wide than 4 mm or 1/2 of the longest diameter of dome. Such geometry makes difficult to contain all loops of a coil in the aneurysm dome, especially when placing a first coil. Loops of a coil tend to herniate into the lumen of parent artery. Several techniques can be applied to avoid such events.

1. **Basket technique :** It is to make a basket covering the neck of aneurysm as well as its dome with a first coil. By adjusting position of a microcatheter and speed of advancing a coil, each loop of coil can be placed in a desired position. An operator has to be familiar with characteristics of coils and monitor advancement of loops carefully. 3D complex shaped coils have been developed to suit in the aneurysm better. It is favorable to use an oversized coil when using this technique. Once a proper basket is made, subsequent smaller size coils can be introduced in the middle of the initial mesh, gradually filling the space/another technique to accomplish similar results is to use multiple catheters. Two or more catheters may be placed in the aneurysm dome, and coils are advanced loop by loop to make a tangled mesh to be more stable and cover neck better.
2. **Piece meal technique :** When aneurysm dome is elongated or lobulated, it may not be possible to cover the neck and dome together with a initial single coil. In such cases, aneurysms have to be treated as more than one compartment. Distal dome is treated separately as one aneurysm. As this compartment becomes packed with coils, several loops of subsequent coils are brought down toward the neck gradually. The first part of newly introduced coil is tangled in the mesh of initial basket which makes it stable in the free empty lumen. Gradual covering of the neck by this technique is safer than attempting to close the neck with a single coil in awkward shaped aneurysms. Two or more microcatheters can be placed in the lumen of an aneurysm and 2 or more coils can be placed to make a secure mesh of coils when a single coil can not make a proper basket.
3. **Neck remodeling technique :** This technique is to prevent herniation of any coil into the parent artery lumen by placing a non-detachable balloon across the neck of aneurysm. It was introduced by Jacques Moret. He mounted a latex detachable balloon on a microcatheter and secured it to be non-detachable. The balloon catheter was placed in the lumen of the parent artery separately across the neck of aneurysm. Following introduction of a microcatheter in the aneurysm lumen, the balloon is inflated while a coil is advanced. The inflated balloon works as a mechanical blocker to keep loops of coil in the aneurysm lumen. Once whole coil is in the aneurysm, the balloon is deflated. The coil is then detached, if there is no movement of coil mesh. In case loops of coil move into the parent artery, it is repositioned, while balloon is re-inflated. This process is repeated as each coil is introduced. This technique provides security while placing individual coils. However, it requires two separate guiding catheters or a larger lumen catheter to accommodate two microcatheters.



- 4. Stent assisted technique :** A self expanding stent has been developed to minimize any possibility of coil loops protruding into the parent artery lumen either during deployment or after detachment of a coil. The principle is to place a metal stent across the neck of aneurysm and then introduce coils so that loops of coil stay in the dome. A few reports of such technique using stents for coronary artery stenoses were published initially. Those stents were rigid and mostly balloon expandable. Therefore, navigation into the desired location in the cerebral circulation was often difficult. In 2000, a self expanding stent system, "Neuroform," specifically designed for wide neck aneurysm treatment was introduced. After brief clinical trial, it was approved by the FDA of United States in 2002 and started commercial distribution as a HDE device. The stent is made of Nitinol, which has property of spontaneous expansion when temperature is elevated. It is so called "open cell" design. Only two corners of diamond shaped opening are connected to maintain integrity of stent shape. It has been more improvement of stent itself as well as delivery system.

Other stent systems have been introduced. "Enterprise" stent system is made of same Nitinol. However, design is different from the "Neuroform" stent. "Enterprise" is "closed-cell" shape. All corners of diamond shaped cell is connected each other. This stent system is more flexible and smoother. The closed cell design allows a stent follow the curve of parent artery and less likely herniated into aneurysm lumen. It also makes almost impossible any loop of coil protrude into the parent artery through cells (opening), since length of cell is 1 mm when it is fully expanded. It is detachable system so that initial position of a stent is not at the intended location, it can be withdrawn to the delivering microcatheter. It allows reposition a stent unless more than 80% length of a stent is deployed. These stents are intended to use of wide neck aneurysms with parent artery ranging from 2 to 4.5 mm in diameter. Other stent systems are available outside of U.S..

- 5. Flow Diverters :** Flow diverters are the second generation of metallic stents for treatment of difficult aneurysms. These have higher metal-surface area coverage, up to 35%. Higher coverage provides sufficient scaffolding for endothelial growth and eventual complete reconstruction over



the aneurysm neck. Early reports showed impressive results of treating difficult wide neck or fusiform aneurysms. There are three different stents are in clinical use now; Pipeline (Covidien, USA), SILK (France) and Surpass (Israel, Europe). All three products have been approved in Europe, however, the Pipeline is the only one approved by FDA of USA. Contrary to awesome results, there have been number of cases of delayed rupture of aneurysms treated with flow diverters. Exact mechanism(s) has not been understood. Several possible explanations were raised. One is shift of inflow zone and shear stress in the wall of aneurysm. Other one is change of intraluminal arterial pressure. However, according to the recent report by Schneiders et al in AJNR (Aug. 18, 2011), intra-aneurysmal pressure stabilizes quickly with arterial pressure of the parent artery. Kulscar et al (AJNR 32: 20-25, Jan. 2011) theorized that thrombus induced autolysis may play a role in weakening wall of aneurysm and eventual rupture. They observed that those ruptured following FD treatment are large or giant in size, recently became symptomatic, saccular aneurysms with wide neck and inertia driven inflow not modified by FD. Recently, some investigators are using detachable coils in conjunction with FD to avoid delayed ruptures.



Dural Arteriovenous Shunts: from diagnosis to treatment

Dong Joon Kim

Department of Radiology, Yonsei University College of Medicine, Korea

Dural arteriovenous shunt is a dynamic disease in which abnormal arteriovenous communications develop within the dura usually within or near the walls of a dural sinus. Many factors have been associated with DAVS formation such as sinus thrombosis, infections, surgery, post partum status, and various coagulopathies. Angiogenic growth factors also seem to be associated in its pathogenesis. About 16% of the patients show spontaneous pattern conversion with sinus thrombosis causing either spontaneous sinus obliteration or aggressive conversion in relation to the underlying venous topography.

The transverse-sigmoid and the cavernous sinuses are the most frequent sites with the cavernous sinus being the most frequent in the Asians. The symptoms of these lesions depend on the location of the shunt, the type of venous drainage, and the flow characteristics.

The presence of cortical venous reflux is an important prognostic feature which is implicated with increased intra-cranial hemorrhagic rates and annual mortality rate of about 10%. Recent studies show that cortical venous reflux accompanied by initial aggressive symptoms is more prone to poor natural history with hemorrhagic rates of 7-8%/year. Curative management is recommended for such lesions. On the other hand, DAVSs without cortical reflux are benign and conservative management consisting of palliative or observational treatment is advocated.

The treatment modalities for DAVS include transarterial embolization using particulate or liquid embolic agents, transvenous embolization using coils, surgical disconnection of cortical reflux, and radiation therapy. In terms of endovascular treatment, angiographic cure rate of transarterial low concentration glue embolization can reach 55% for Borden type III lesions. Transarterial onyx embolization is known to show cure rates of 60-90%. Transvenous coil embolization results in sacrifice of the venous sinus with angiographic cure rate ranging between 70-88%.





E-Poster

*Abstract No. A1*

Consecutive Performance of CT Perfusion and CT Angiographic Surface Anatomic Scanning of Brain Tumors

K. Tsuchiya, M. Imai, H. Tateishi, T. Nitatori

Kyorin University, Mitaka, Tokyo, Japan

BACKGROUND: CT perfusion (CTP) has been an established technique to evaluate the tumor hemodynamics.

OBJECTIVE: We assessed the feasibility and value of consecutive acquisition of CTP and CT angiographic surface anatomic scanning (CTA-SAS) of brain tumors.

METHODS: We examined 48 cases of preoperative brain tumor (4 of low-grade glioma [LGG], 16 of high-grade glioma [HGG], 8 of meningioma, 7 of metastasis, 2 of lymphoma, and 11 of others) on a 64-row CT. First, we performed a whole-brain precontrast scan followed by CTP using 25 mL of contrast agent (350 mgI/mL). Next, CT angiography (CTA) was obtained using 75 mL of contrast agent. In postprocessing, we first generated CTP maps of cerebral blood volume/flow (CBV/CBF) and a mean transit time. Then, we generated CTA images, created surface images by removing the skull and scalp, and combined the two kinds of images to produce CTA-SAS. CTP maps were assessed using a 3-point grading scale regarding tumor vascularity. We assessed CTA and CTA-SAS images regarding demonstration of the tumor, other vascular lesions, and adjacent brain structures.

RESULTS: In all cases, we could obtain CTP maps. Cases of metastasis, meningioma, and schwannoma showed hyperperfusion (CBV + CBF: 5 points or more), while those of LGG and lymphoma showed hypoperfusion (CBV + CBF: 4 points or less). Among the 16 cases of HGG, 14 showed hyperperfusion. CT angiograms depicted tumor vascularity in 17 cases, while they demonstrated a vascular lesion in 7 cases (aneurysm in 5 and focal stenosis in 2). CTA-SAS visualized gyri, sulci, and adjacent vessels in all cases in correspondence with operative findings. The tumor was variously depicted depending on the histology.

CONCLUSIONS: CTP and CTA-SAS can be performed consecutively. They provide images that facilitate the differential diagnosis and yield information about adjacent brain surface anatomy as well as vascular lesions.

Abstract No. A2

Feasibility and Usefulness of Apparent Diffusion Coefficient at 3T for Differentiating Benign from Malignant Tumors of the Head and Neck

Maeda M, Umino M, Matsushima N, Takeda K

Department of Radiology, Mie University School of Medicine, Tsu, Japan

BACKGROUND: Although susceptibility artifacts can affect echo-planar DWI (EPDWI) images more strongly at 3 T, it has come to be used instead of 1.5 T for the head and neck. Therefore, we must determine the feasibility and the usefulness of EPDWI at 3 T.

OBJECTIVE: The purpose was to evaluate the feasibility of DWI of head and neck tumors and to assess the usefulness of the apparent diffusion coefficient (ADC) for differentiating benign from malignant tumors at 3 T.

METHODS: In total, 56 patients with head and neck tumors were examined. The tumor pathology included benign entities (n=23) and malignant entities (n=33). MR imaging was performed using a 16-channel neurovascular coil on a 3T MR scanner (Achieva; Philips Co.). DWI was conducted with single-shot SE EPDWI fat-suppressed with STIR. The ADC of benign and malignant tumors were calculated and compared.

RESULTS: Among 56 cases, three (5.3%) were not able to be evaluated on DWI because of susceptibility artifacts (denture or air). Those cases included tumors of gingiva (n=2) and the nasal cavity (n=1). In the remaining 53 cases, the DWI images and the ADC were sufficiently evaluated without remarkable artifacts. The ADC was $0.90 \pm 0.18 \times 10^{-3} \text{ mm}^2/\text{s}$ in malignant tumors; it was $1.45 \pm 0.34 \times 10^{-3} \text{ mm}^2/\text{s}$ in benign tumors. A significant difference was found between the two ($p < 0.005$). When the cut-off value of $1.14 \times 10^{-3} \text{ mm}^2/\text{s}$ was used for differentiation, the sensitivity and specificity were, respectively, 78.9% and 92.6%.

CONCLUSIONS: The 3T MR imaging was overall feasible for evaluation of DWI and ADC of head and neck tumors, although 5.3% of cases were not possible for the evaluation because of susceptibility artifacts. Our results suggest that the ADC was useful to differentiate benign from malignant tumors of the head and neck at 3T.

*Abstract No.A3*

MR voxel based Histogram Analysis of Atherosclerotic Basilar Artery in patients with Isolated Pontine Infarction

H.W Jang^a, H.J. Lee^b, S.W. Yoon^c

Daekyung Radiology clinics^a, Daegu, Republic of Korea^b

Department of Radiology, Kyungpook National University Hospital, Daegu, Republic of Korea^b Department of Radiology,

School of Medicine, Catholic University of Daegu, Daegu, Republic of Korea^c

Background and Objective: Each voxel magnetic resonance imaging of atherosclerotic vessels represents various tissue components of atherosclerotic plaque according to the physical property of the corresponding tissue. We hypothesized the pattern of magnetic resonance voxel based Histogram (MRH) represent atherosclerotic status.

Methods: 42 consecutive patients (26 male patients and 16 female patients; age range, 44 to 85 years) with an acute isolated pontine infarction. Using our own program (CI image, version 1.0), we analyzed voxel data and calculated the numbers of voxels according to signal intensities from the T1 weighted and T2 weighted HRMRI of basilar arterial wall in 42 patients diagnosed with acute isolated pontine infarction and 10 normal healthy volunteers. From the data we obtained the MRH in relation to signal intensities. We defined each peak into P[lumen], P [wall], P[cistern], and P[brain parenchyma]. We compared the patterns of histogram according to the presence steno-occlusive lesions of basilar arteries.

Results: The spectra from the normal healthy control group showed two phasic peaks for T1 weighted images and multi phasic peaks from T2 weighed images. The spectra from the steno occlusive disease group showed decreased height of the peak from area of the luminal signal void and increased peak from the atherosclerotic plaques. The ratio of P[wall]/P[lumen] were higher in steno-occlusive disease group on spectrum form T1WI (2.47 versus 1.06, $p<0.001$) and T2WI (1.22 versus 0.71, $p<0.001$).

Conclusions: This study demonstrated that HRH of basilar arteries in patients with isolated pontine infarction. We thought this method could give the quantitative information for the status of atherosclerosis.

Abstract No. A4

A Case of Cystic Lesion on FLAIR MR Images of the Temporomandibular Joint (TMJ)

Otonari-Yamamoto M, Imoto K, Sakamoto J, Yamamoto A,
Kodama S, Yonezu H², Abe S³, Shibahara T⁴, Sano T.

Department of Oral and Maxillofacial Radiology, Tokyo Dental College, Chiba, Japan.

²*Department of plastic, Oral and Maxillofacial Surgery, Teikyo University School of Medicine, Tokyo, Japan.*

³*Department of Anatomy, Tokyo Dental College, Chiba, Japan.*

⁴*Department of Oral and Maxillofacial Surgery, Tokyo Dental College, Chiba, Japan*

BACKGROUND: Synovial cysts can occur in the joints but the cyst arising in the TMJ is rare. We routinely perform FLAIR technique for MRI of TMJ.

OBJECTIVE: To introduce a case of cystic lesion that FLAIR technique was feasible for differential diagnosis in the TMJ.

CASE: A 23 year-old man visited our hospital with complaint of pain in the right temporomandibular region. Though medication and physical therapy were performed for three months, the symptom did not make changes. MRI was performed and revealed a mass in fat tissue at postero-lateral to the right TMJ capsule. It showed low signal on T1W, high signal on T2W, and lower signal than fat tissue did on PDW. A synovial cyst was suspected because the continuity of the lesion to the upper joint space was suspected on PDW. Vascular lesion was also suspected. Since the differential diagnosis between both suspected lesions was difficult only with PDW and T2W images, we used FLAIR images to analyze the element of the lesion. The suppression ratio of the signal intensity by FLAIR was calculated. The suppression ratio of the lesion (28.38%) was similar to that of joint fluid (36.17%), lower than that of CSF (70.73%), and higher than that of blood vessel (-73.93%). it was suggested the lesion would be a synovial cyst.

*Abstract No. A5*

MRI study of Intracranial Hydrodynamic and Ventriculoperitoneal Shunt Responsiveness in Patient with Normal Pressure Hydrocephalus.

**Theerapol Witthiwej², Pathomlirk Sathira-ankul²,
Panida Charnchaowanish¹, Orasa Chawalparit¹**

¹Department of Radiology, Surgery, ²Faculty of Medicine Siriraj Hospital, Mahidol University, Bangkok, Thailand.

OBJECTIVE: To determine the predictor for shunt responsive cases in patient with normal pressure hydrocephalus (NPH) by means of MRI CSF flow study at Siriraj hospital.

MATERIAL AND METHODS: The retrospective study was performed in patients suspected NPH and underwent MRI CSF flow measurement. 2D-phase contrast technique (Achieva, 3 Tesla Philips system) was used as CSF flow analysis. The preoperative and postoperative clinical outcome were collected and analyzed to determine predictive value of MRI CSF flow measurement in shunt responsive patients.

RESULTS: During 5 years periods (2006-2011), twenty NPH patients were treated by ventriculoperitoneal shunt placement. Fourteen of 20 cases had improved, at least in gait score. Of these, 10 were defined as significant responsive group for overall improvement of outcome (sum of Japanese NPH score ≥ 3). The mean velocity of the CSF flow through the aqueduct of Sylvius was significant difference between shunt-responsive and non-responsive groups ($p < 0.05$); the peak velocity was significant difference between gait responsive and non-responsive groups ($p < 0.05$). Using a mean velocity threshold 26 mm/sec to identify the significant responsive group, the sensitivity was 50%, specificity 83.3%, positive predictive value 87.5% and accuracy 70%. In order to identify the gait responsive group by using a threshold of peak velocity 70 mm/sec, the sensitivity was 60%, specificity 83.3%, positive predictive value 81.5% and accuracy 60%.

CONCLUSION: Using available commercial software in the authors' institute, the mean velocity as well as the peak velocity was a specific value which predicted significant shunt responsiveness in NPH patients.



Abstract No. A6

Congenital External Carotid-Internal Carotid Artery Anastomosis Diagnosed By MR Angiography

A. Uchino, N. Saito, T. Watadani

Department of Diagnostic Radiology, Saitama Medical University International Medical Center, Hidaka, Saitama, Japan

BACKGROUND: Rarely, the major branches of the proximal external carotid artery (ECA) arise separately from the terminal segment of the common carotid artery or proximal internal carotid artery (ICA) so that the ECA has no proximal main trunk. This anomaly is called a non-bifurcating cervical carotid artery and may be caused by segmental agenesis of the most proximal ICA. We report a case of congenital EC- IC anastomosis at the cervical segment that forms a large arterial ring. This seems to be a variant of the non-bifurcating cervical carotid artery. To our knowledge, no similar cases have been reported.

CASE REPORT: An 89-year-old man with acute cerebral infarctions underwent emergency cerebral magnetic resonance (MR) imaging and cerebral MR angiography that included the cervical carotid bifurcation. MR angiography showed occlusion of the left vertebral artery. The left carotid bifurcation was located at the level of C4/5 intervertebral space, and the proximal cervical segment of the left ICA was small in caliber, whereas the left proximal ECA was large. The 2 arterial branches anastomosed at the mid-cervical segment to form a large arterial ring at the proximal cervical segment. The patient was treated conservatively.

CONCLUSION: We present what we believe is the first report of EC-IC anastomosis, which forms a large arterial ring at the proximal cervical ICA. If the small channel of the proximal cervical ICA is occluded, the remaining large channel of the external carotid artery may be diagnosed as a non-bifurcating cervical carotid artery.

*Abstract No. A7*

Fractional Anisotropy by Diffusion Tensor Imaging in Thai Populations

Ittimakin S., Lerdlum S.

Department of the Radiology, King Chulalongkorn Memorial Hospital, Bangkok, Thailand

BACKGROUND: Diffusion tensor imaging (DTI) is a new MRI technique that recently uses in several neuropsychiatric diseases e.g. white matter tract disease, schizophrenia, neurodegenerative disease and some infectious disease. Quantification of DTI is represented into several value, mainly fractional anisotropy (FA), mean diffusivity (MD) etc.

OBJECTIVES: To prospectively determine FA value at the different brain regions of normal Thai population and to determine relationship between aging and FA value in each brain regions.

METHODS: Institutional review board approval and informed consent were obtained. Fourteen normal patients who age more than 40 years (mean age 71.6 years) and eleven normal patients who age between 20-40 years (mean age 28.1 years) underwent diffusion tensor image study with a 1.5 Tesla magnetic resonance system. An echo-planar imaging diffusion sequence was used with 25-direction technique and a twelve-channel head coil. The mean fractional anisotropy (FA) of several white matter (WM) regions were determined. Descriptive data (mean \pm SD) of the FA value in each brain regions were demonstrated. Single posttest comparisons were performed with the student t-test, with an overall statistical significance level of 0 .05.

RESULTS: Total 25 subjects were included in this study, 11 subjects of the young adult and 14 subjects of aging group. The FA values is high at the area of thick nerve fiber e.g. corpus callosum, anterior and posterior cingulum. There is significant decreased FA value of aging group at the splenium of corpus callosum, frontal white matter, occipital white matter and left posterior cingulum as compared to the young adult group.

CONCLUSIONS: The FA value in each brain regions that can use to compare with the patients who suspected white matter disease. There is significant correlation between age and FA value at the specific regions from DTI.

Abstract No. A8

Magnetic Resonance Measurement of Total Intracranial Volume Among Malay Population: Accuracy of Alternative Measurement Methods.

Win Mar @ Salmah J, B Musa, M S Abdullah, A H A Kareem

Department of Radiology, Hospital Universiti Sains Malaysia, USM, Kubang Kerian, Kelantan, Malaysia

BACKGROUND: Total intracranial volume (TIV) is defined as the volume within the cranium, including the brain, meninges and cerebrospinal fluid. It provides a stable and accurate normalization factor for other brain structures. Accurate measurements are possible by advanced magnetic resonance (MR) technology. There were various methods of MR volumetry and manual method is the best. The standard method measures all slices covering the whole brain and is time consuming. Therefore a method which has less time consuming without affecting the accuracy and reliability is necessary.

OBJECTIVES: To compare the accuracy of MR volumetry of TIV using two alternative methods with the standard method.

METHOD: This was a cross sectional comparative retrospective study of TIV using alternative and standard method among normal Malay population. A total of 59 (32 females, 27 males) subjects, age ranged from 15 to 50 years were included. Measurement was performed manually on sagittal T1 images using Osiri X version 3.2.1. Three different methods were done; 1. Standard Method measured all the slices; 2. Alternate Slice Method measured one alternate slices and 3. Half Cranial Method measured right and left half of ICV. The mean and standard deviation (SD) of TIV by all methods were analyzed and compared. Mean difference of TIV between genders were also calculated.

RESULTS: Mean TICV for all subjects was 1375.67 (148.61) cm³, for male and female were 1439.14 (142.49) cm³ and 1322.12 (133.12) cm³ respectively. Male and female TICV were significantly different ($p = 0.002$) with male being larger. There were high reliability and agreement between the alternative and standard methods. The intraclass correlation coefficient (ICC) for TIV from each alternative method (right and left half TIV, alternate slice TIV) and standard method were ranging from 0.977 to 0.981 and the Cronbach's Alpha was 0.991.

CONCLUSION: The alternative methods are accurate, reliable and less time consuming.

*Abstract No.A9*

MRI-Based Localization of Intractable Hiccup after Acute Lateral Medullary Infarction

Yoo BG¹, Kim MK¹, Jang YS²

¹*Department of Neurology, Kosin University College of Medicine, Busan, Korea*

²*Department of Neurology, Busan Adventist Hospital, Busan, Korea**

BACKGROUND: Intractable hiccups are defined as hiccup persisting for more than 48 hours. The relationship between lesion location of lateral medullary infarction (LMI) and intractable hiccup is rarely reported. Objective: This study was designed to investigate the MR localization of intractable hiccups in the LMI.

METHODS: We identified 9 patients with intractable hiccups by medical record, telephone interview and brain MRI. LMI was diagnosed by clinical findings and brain MRI. MRI lesions were classified vertically as upper, middle and lower level and horizontally.

RESULTS: All patients with intractable hiccups were men. Vertically, three patients had lesions in the upper medulla, two patients had lesions in the upper and middle medulla, two patients had lesions in the all levels of the medulla, one patient had lesions in the middle medulla, and one patient had lesions in the middle and lower medulla. Horizontally, dorsolateral and/or midlateral lesions were always involved. All patients with LMI with intractable hiccup had vertigo/dizziness, nausea/vomiting and dysphagia.

CONCLUSIONS: These results demonstrate that intractable hiccups are related to the dorsolateral region of the middle and/or upper levels of medulla. We suggest that involvement of the nucleus ambiguus may be responsible for intractable hiccups.



Abstract No.A10

DYNA CT AND B-AVM

UR Chaudhry, S.K. Bhatti, M. Farooq

Department of Interventional Neuroradiology, Lahore General Hospital/Post Graduate medical Institute, Lahore, Pakistan

BACKGROUND AND OBJECTIVES: The purpose of this study is to evaluate the use of syngo Dyna CT, a flat panel biplane angiography system by Siemens, Eelangen, Germany with 3 D reconstruction and cone beam Ct scan in obtaining information from intra arterial injection of contrast to show the detail of intracerebral AVM which was not as well demonstrated on the routine 2D angio. All of this information is important in understanding the vessel architecture of the AVM and determining the associated risk of bleeding.

MATERIAL AND METHODS: Total of 10 patients with diagnosed AVM by MRI or CT were taken and conventional 2D angiography was done to confirm the diagnosis. To know the further anatomical details 3D rotational angiography was performed using Dyna CT/Flat Panel detectors by Siemens Medical systems Germany. In 7 patients (70%) the bleeding site could be appreciated. In 02 patients (20%) intra or post nidal aneurysm visualized which was not visualized in conventional study. It also provides detailed information about its location.

RESULTS: With the help of 3D rotational angiography syngo Dyna CT showed the anatomic locations of the AVM in the brain, their arterial supply, venous drainage and relationship to surrounding structures. Greater details of pre, intra or post nidal aneurysms appreciated along with localization of bleeding site which is of great help in treatment planning.

CONCLUSIONS: Dyna CTA can be an easy and effective technique for the evaluation of the detailed anatomy of AVM, which cannot be provided with any of the existing radiological investigation. It can also serve as a guide line for not only the diagnosis but also for the treatment planning and to localize intra procedural complications without mobilizing the patient out of angiography suit.



Abstract No.A11

Microstructural Change of the Brain in Chronic Obstructive Pulmonary Disease: a Voxel-based Investigation by MRI

WS Choi¹, C Ryu¹, G Jahng¹, H Rhee², CW Choi³, MJ Kim¹

¹Department of Radiology, School of Medicine, Kyung Hee University, Seoul, South Korea.

²Department of Neurology, School of Medicine, Kyung Hee University, Seoul, South Korea.

³Department of Internal Medicine, School of Medicine, Kyung Hee University, Seoul, South Korea

BACKGROUND: A cognitive deficit is a common problem in patients with chronic obstructive pulmonary disease (COPD). We presumed that fiber integrity and structural volumetric MRI measures may allow improving of our understanding and quantification of the progression of the neuronal damage in COPD in vivo.

OBJECTIVE: To prospectively evaluate if MRI can demonstrate the microstructural volume loss and the diffusion anisotropic change in subjects with COPD, compared with cognitively normal (CN) subjects.

METHODS: Institutional review board approval and informed consent were obtained. Six subjects with severe COPD (6 men, mean age, 69.8 years), 13 with moderate COPD (12 men, 1 women; mean age, 65.3 years), and 12 CN subjects (12 men, mean age, 63.9 years) underwent isotropic volumetric T1-weighted imaging and diffusion tensor imaging (DTI) with 32 directions and b-values of 0 and 800 sec/mm². Pre-processing steps were performed with SPM5 software and voxel-based statistical analyses among groups were performed on brain volumes, fractional anisotropy (FA) and trace. Cognitive function tests (CFT) were performed in all subjects, and the CFT scores were compared among three groups.

RESULTS: There wasn't any significant regional difference of gray matter in both severe and moderate COPD groups compared with normal control group. For FA between severe COPD and CN or between severe and moderate COPD, FA reduced extensively in both the cerebral cortex, frontoparietal periventricular white matter and the corticospinal tract. The trace value of the moderate COPD group was significantly higher in bilateral occipital cortices, left hippocampus and left superior frontal cortex than the NC group. The regions with increased trace in COPD groups were matched with the region with decreased FA in COPD compared with CN. The severe COPD group showed significantly lower score in the language-related function, visuospatial function and frontal executive function than the CN and moderate COPD group (Kruskal-Wallis test <0.05), and CFT scores did not show any significant differences between CN and moderate COPD.

CONCLUSIONS: This study demonstrated that COPD patients could affect the axonal integrity in multiple brain regions. The result of this study suggested the severity of COPD and the cognitive function might be correlated with the extent of microstructural change in brain. Voxel-based evaluation by MRI may be useful for preclinical detections of the cognitive dysfunction in patients with COPD.

Abstract No.A12

CT Perfusion and CT Angiography Analysis in Acute Stroke

**Syazarina S¹, Abdul Rashid Misran¹, Shahizon M¹, Husyairi H²,
Zuraidah CM², Wan Nur Nafisah³, Ahmad Sobri Muda¹**

¹Radiology Department, ²Emergency Department, ³Neurology Department,

Universiti Kebangsaan Malaysia Medical Centre, Kuala Lumpur

We have started our acute stroke treatment programme in 2010 following the formation of KRISIS (KL Regionalized Integrated Stroke Intervention Strategy) in 2009. All acute stroke patients who meet the criteria for revascularization either via IV thrombolysis or mechanical thrombolysis will undergo perfusion and angiography preferably using CT to evaluate presence of penumbra or salvageable area for thrombolysis. The criteria include NIHSS score of not less than 5, arrival in Emergency Department within 6 hours and no other contraindication for thrombolysis. All intent to treat patients will undergo CT perfusion with CT angiography unless contraindicated for CT, where patient will have MR stroke protocol with or without MR perfusion.

As the decision of treatment in our centre is a collective decision lead by neurologist in consultation with neuroradiologist and emergency physician, perfusion and angiography findings [within 45 minutes door to perfusion findings] are among important information. We describe the analysis of our early experience in perfusion scan for intent to treat patients in acute stroke.



Abstract No.C1

Audit of Appropriateness and Outcome of Computed Tomography Brain Scanning for Headaches in Pediatric Age Group

Muhammad Nawaz

Radiology Department Hayatabad Medical Complex, Peshawar Pakistan

OBJECTIVE: To assess the appropriateness and outcomes of computed tomography brain scanning for headaches in pediatrics age group.

MATERIAL AND METHODS: This Descriptive study was conducted at the Radiology Department Hayatabad Medical Complex, Peshawar over a period of 1 year i.e. from 9-07-08 to 9-07-09. Patients of both genders between the ages of 4-18 years presenting with headache either isolated or common/classic migraine were included in this study. These variants of headache were allocated an appropriateness rating of 2 for CT scan by the American College of Radiology Appropriateness Criteria (ACRAC) for children with headaches.

RESULTS: Out of the 100 patients only 4% patients showed abnormal findings on CT scan while the remaining 96% of the scans were absolutely normal. The four patients with abnormal findings all had sinusitis.

CONCLUSION: This audit suggests that a proportion of the computed tomography studies performed for children with isolated headaches or common/classic migraine may have been inappropriate. The development of a local guideline for imaging referral is indicated.

Abstract No.C2

Imaging in Migraine - A Pictorial Essay

S Agarwal, Associate Professor,

Department of Radiodiagnosis, Pandit Bhagwat Dayal. Sharma,

Post Graduate Institute of Medical Sciences, Rohtak (Haryana) India.

BACKGROUND: Migraine is a common and chronic disorder. It is a debilitating primary headache disorder that is ranked by the World Health Organization as the 19th among all causes of years lived with disability. Its prevalence varies from country to country and occurs in 5% to 20% of the population. It is usually considered benign, however it has been suggested as a risk factor for the development of infarcts and infarct-like lesions in the territory of posterior circulation. Reversible white matter abnormalities, vasospasm on angiograms and fatal migranous infarctions have all been reported in the literature. The true etiology of these lesions is still a matter of debate. Various mechanisms have been postulated including altered perfusion pressures and activation of the clotting and endothelin systems leading to vasoconstriction, thrombosis and resultant ischemia, however the underlying mechanism is still not clear.

MATERIAL AND METHODS: I will be presenting my experience with imaging of patients with migraine as a pictorial essay with both isolated white matter lesions and reversible lesions.

CONCLUSION: These lesions can cause apprehension in the mind of the sufferers and the treating physicians. Hence it is important to correctly diagnose these lesions and make the patient aware of the prognosis associated with these lesions.



Abstract No.C3

New And Rare Congenital Anomalies Everyday: Are We To Blame?

S Agarwal M.D, D.N.B, G Gathwala M.D, D.M, K Mittal

Department of Radiology and Pediatrics, Pandit Bhagwat Dayal Sharma,

Post Graduate Institute of Medical Sciences, Rohtak (Haryana) India.

ABSTRACT: Great advances have been made in the field of diagnosis and management of congenital anomalies during the last decade, yet new and rare congenital anomalies continue to be discovered. We present the imaging findings of a series of such central nervous system (CNS) structural anomalies diagnosed in our department over a 06 year period that is may 2005 to may 2011.

MATERIAL AND METHODS: Seven structural congenital CNS anomalies were observed during this period. These were, third cerebellar hemisphere, anterior thoracic myelomeningocele presenting as an abdominal mass, unilateral hypoplastic internal auditory meatus (IAC) with agenesis of facial and vestibulochochlear nerve presenting as congenital facial palsy, isolated agenesis of facial nerve presenting as congenital facial palsy, bilateral agenesis of oculomotor nerve presenting as bilateral ptosis, antenatal otocephaly and antenatal conjoined twins. All the anomalies were missed on other imaging modalities and a diagnosis could be made only on magnetic resonance imaging (MRI).

CONCLUSION: Magnetic resonance imaging is the modality of choice for diagnosing structural CNS anomalies whether it in the antenatal period or the postnatal period. This makes us wonder whether discovery of new and rare anomalies everyday is because of advancement or is it the result. For all we know it could be a part of evolution.

Abstract No.C4

Radiologic Manifestation of Multiple Solitary Plasmacytomas: a Case Report

Yueniwati Y, Erawati DR, Arisetijono M

Radiology Department, Faculty of Medicine, University of Brawijaya, Malang - East Java - Indonesia

Plasmacytoma, a neoplastic proliferation of plasma cells, is one form of plasma cell dyscrasia that may manifest as multiple myeloma, primary amyloidosis, or monoclonal gammopathy of unknown significance. Plasmacytoma may be primary or secondary to disseminated multiple myeloma and may arise from osseous (medullary) or nonosseous (extramedullary) sites. Primary extramedullary plasmacytoma can be solitary or multiple. Commonly occur in adult more than 50 years old. Multiple solitary plasmacytomas are rare manifestations of plasma cell tumors. A 37-year old man came to our hospital with severe anemia because of chronic-residive mouth bleeding. He also had got multiple mass on his head and cheek since 6 month before. Bone survey revealed multiple osteolytic lesions in skull, mandible, proximal upper limb, and osteolytic-destructive in thoracic cage dan thoracolumbar vertebrae. Chest CT scan confirmed that multiple osteolytic lesions in ribs and thoracal vertebrae. MRI showed multiple bone lesions in mandible and skull with slight compression to the brain. According to FNAB in cheek and thoracic cage mass, it was plasmacytoma. BMP showed that the number of plasma cells didn't increase significantly, so it wasn't confirmed as multiple myeloma. The purpose of this report is to study the imaging features and role of imaging in multiple solitary plasmacytoma, therefore radiologist can aware early imaging of multiple solitary plasmacytoma.



Abstract No.C5

Coordination between the Categorical Reporting Systems for Cytologic results and Ultrasonographic Findings in Determination of Repeat Fine Needle Aspiration Biopsy for Thyroid Nodules

HJ Lee^a, HJ Kim^a, JY Park^b, HK Kim^c, HW Jang^d

Department of Radiology, Kyungpook National University Hospital^a

Department of Pathology, Kyungpook National University Hospital^b

Department of Radiology, School of Medicine, Catholic University of Daegu, Daegu,

Republic of Korea^c Daekyung Radiology clinics^a, Daegu, Republic of Korea^d

OBJECTIVE: Our goal was to investigate the usefulness of the coordination of the categorical reporting system for cytologic results and Ultrasonographic findings to suggest indications of repeat US guided Fine needle aspiration (USFNAB).

MATERIAL AND METHODS: 342 patients (316 female, 26 male) who went through repeated US guided FNAB of thyroid nodules were included in the cohort study. Results of FNAB (THY1, inadequate; THY2, benign; THY3, indeterminate; THY4, suspicious malignant; THY5, malignant), and US findings (THY1, inadequate; THY2, benign; THY3, indeterminate; THY4, suspicious malignant; THY5, malignant) were classified to five grades and evaluated. The grades of initial FNAB and US findings were further divided to simplified high risk and low risk groups. The frequency of malignant nodule was evaluated by Kaplan-Meier method and Cox proportional risk model in each grade. The sensitivity, specificity and accuracy were evaluated as malignant nodules when the patient was the high-risk group of initial FNAB or US findings.

RESULT: Cox proportional risk model of FNAB results and US findings revealed significant relative risk ratio of 1.6 for THY1, 9.3 for THY3 compared to THY2, and 6.2 for TUS3, 8.3 for TUS4, 10.4 for TUS5 compared to TUS2. THY1 and THY3 of FNAB findings and 3, 4, 5 grades of US findings were high malignancy rate than others and would be regarded as high-risk group. The sensitivity, specificity, positive predictive value, negative predictive value and accuracy were 79.2%, 91.7%, 63.6%, 96.0% and 89.8%, if nodule was high risk group of FNAB or US findings ($p < 0.05$).

CONCLUSION: The coordination between the categorical reporting system for cytologic results and Ultrasonographic findings could be useful to suggest indications of repeat USFNA.

Abstract No.C6

Target sign in CNS Toxoplasmosis : The value of T1 post contrast 3D MPRAGE

Shahizon M, Sobri M, Syazarina S, Redzuan I

Department of Radiology, Universiti Kebangsaan of Malaysia Medical Centre, Cheras, 56000 Kuala Lumpur, Malaysia

OBJECTIVE: To demonstrate a new imaging observation of central nervous system (CNS) toxoplasmosis. Cerebral toxoplasmosis remains one of the most common focal brain lesions in patients with acquired immune deficiency syndrome (AIDS). Diagnosis is a challenge because on cranial imaging it closely mimics CNS lymphoma, primary and metastatic CNS tumors, or other intracranial infections like tuberculoma or abscesses. The target sign has been used as radiologic descriptor for toxoplasmosis and other infective causes.

We report three cases of CNS toxoplasmosis with magnetic resonance imaging (MRI) evidence of target lesion. We also reviews previously described and fairly well-known target sign seen in toxoplasmosis. In addition, we attempt to add to diagnostic armamentarium in CNS toxoplasmosis by describing the new imaging observation of "prominent vessels extending from the central core of target lesion" best depicted in post contrast three-dimensional magnetization-prepared rapid acquisition with gradient echo (3D MPRAGE).

CONCLUSION: High resolution 3D MPRAGE sequence is valuable in demonstrating the new findings of "prominent vessels extending from the central core of target lesion" in cerebral toxoplasmosis, which, when present, can help make the diagnosis of toxoplasmosis.

*Abstract No.C7*

Anomalous Origin Of The Occipital Artery Diagnosed by Magnetic Resonance Angiography

A. Uchino, N. Saito, W. Mizukoshi, Y. Okada

Department of Diagnostic Radiology, Saitama Medical University International Medical Center, Hidaka, Saitama, Japan

BACKGROUND: It is well known that the occipital artery (OA) can arise from the internal carotid artery (ICA) or vertebral artery (VA). However, the incidence of an anomalously originating OA has not been reported. We investigate its incidence and characteristic features on magnetic resonance (MR) angiography.

OBJECTIVE & METHODS: We retrospectively reviewed MR angiography images that included the carotid bifurcation of 2,866 patients; images were obtained using a standard non-contrast MR angiography protocol and two 1.5-tesla MR units (Achieva Nova Dual, Philips Medical Systems; and Magnetom Avanto, Siemens Medical Systems).

RESULTS: We diagnosed 6 cases (7 arteries) of anomalously originating OA, which represented an incidence of 0.21%. Non-bifurcating cervical carotid artery was not included in these patients. The OA arose from the posterior (3), anterior, or medial aspect of the proximal ICA in 4 patients (5 arteries), from the carotid bifurcation in one, and from the VA in one. Five of the 7 arteries occurred on the right. No patients had associated cerebral arterial variations/anomalies. Neither computed tomography angiography nor catheter angiography was performed in these 6 cases.

CONCLUSION: Anomalously originating OA is rare and occurs with right-side predominance. Correct diagnosis of this variation by MR angiography is important before or during cerebral angiography, especially when selective catheterization to the OA is required.



Abstract No.C8

Bilateral Persistent Trigeminal Artery Variants Diagnosed by MR Angiography

A. Uchino

Department of Diagnostic Radiology, Saitama Medical University International Medical Center, Hidaka, Saitama, Japan

BACKGROUND: A persistent trigeminal artery (PTA) is the most common anastomosis between the carotid and vertebrobasilar system. A PTA variant (PTAV) is an anomaly in which the cerebellar artery arises from the internal carotid artery (ICA) without connection with the basilar artery (BA). In a large MR angiographic series, the prevalence of PTAVs was reported to be 0.34%. The most frequent artery arises is the anterior inferior cerebellar artery (AICA). I present what I believe is the first report of bilateral PTAVs diagnosed using magnetic resonance (MR) angiography and briefly discuss the embryology of this rare anomaly.

CASE REPORT: An 81-year-old woman with small infarctions underwent cerebral MR imaging and MR angiography with a 1.5-tesla imager for the evaluation of brain lesions. MR angiography was obtained using the standard non-contrast 3-dimensional time-of-flight technique. MR angiographic demonstration of bilateral AICAs arising from the precavernous segment of the ICA without anastomosis to the BA indicated bilateral PTAVs.

CONCLUSIONS: The PTAV seems to result from the persistence of the proximal segment of the trigeminal artery associated with an incomplete fusion with the longitudinal neural arteries. This is the first report of bilateral PTAVs diagnosed by MR angiography. If bilateral PTAVs occur independently, literature review indicates an estimated prevalence of bilateral PTAVs is about 0.0012%.



Abstract No.C9

CT and MR Imaging of Congenital and Acquired Hearing Loss: Pictorial Review

Chih-Chun Wu¹, Wan-Yuo Guo², Gong-Yau Lan¹

¹Cheng Hsin General Hospital, Taipei, Taiwan(ROC), ²Taipei Veteran General Hospital, Taipei, Taiwan (ROC)

BACKGROUND/OBJECTIVE:

- 1) To make an educational review of normal ear anatomy, including middle and inner ear structures and cranial nerves at the vicinity with reference to CT and MR imaging.
- 2) To illustrate a spectrum of various causes of congenital and acquired hearing loss on the images.

METHODS:

- 1) A detailed pictorial depiction of normal anatomy with schematic drawing.
- 2) Imaging features of various causes of congenital and acquired hearing loss.

RESULTS: We will present illustrative cases as followed:

- (1) Congenital: Cochlear nerve deficiency, Mondini deformity, Common cavity deformity, Large vestibular aqueduct/sac syndrome, Microtia with absence of external ear, lateral vestibular aqueduct dysplasia, and prenatal infection
- (2) Acquired: Cochlear otosclerosis, cranial nerve VIII neuroma, facial nerve schwannoma, glomus jugulotympanicum, cholesteatomawith auto evacuation

CONCLUSION: This comprehensive review will provide key anatomical information of normal temporal bone, and characteristics of several important pathological conditions of hearing loss on both CT and MR images.



Abstract No.C10

MRI Findings of Toxoplasmosis in Low CD4 Count: Retrospective Analysis

**Zuhanis¹, SI Yun¹, Aida AA¹, Noor Aida Mat Daud¹,
Arvin R¹, Ropiah¹, Christopher Lee², Ahmad Sobri Muda³**

¹Radiology Department, Hospital Sungai Buloh, Selangor

²Infectious Disease Department, Hospital Sungai Buloh, Selangor

³Radiology Department, Universiti Kebangsaan Malaysia Medical Centre, Kuala Lumpur

The incidences of Toxoplasmosis in HIV patients are relatively common. In many of the cases, their presentations and neuroimaging features are atypical, more so in cases of low CD4 count. The neuroimaging features sometime overlap with other infections in the like of tuberculosis or atypical infections or lymphoma.

We analyses MRI findings in patients with confirmed diagnosis of Toxoplasmosis who have CD4 count of 250 or less, between July 2008 to June 2011. We illustrate the typical features and common MRI findings.



Abstract No.11

Flow Dynamic Angioarchitectures, Clinical Manifestations and Endovascular Remodeling of the Galenic Venous Malformations and Dilatation in Tokyo

Y. IIZUKA, M.IWASAKI, M.OOOKA, M.HASEGAWA, N. MURATA, T. GOMI, M. NAGAMOTO, E. KOHDA,

Department of Radiology, Toho University Ohashi Medical Center, Tokyo, Japan

PURPOSE: We present our clinical experience in diagnosis and treatment of Galenic venous malformation (GVM) and Galenic venous dilatation (GVD), with an emphasis on morphological classification, symptomatic algorithm, endovascular strategies, factors affecting treatment.

MATERIALS AND METHODS: Angioarchitecture, imaging findings, clinical symptoms in six GVD cases and twenty-one GVM cases were analyzed. Patient age at diagnosis ranged from prenatal to 28 years old. There were eighteen boys and nine girls. Three patients with GVD and eighteen patients with GVM were treated by transarterial embolization with N- butyl cyanoacrylate. Two cases of choroidal GVM were managed by transarterial glue embolization and transvenous coil embolization. We also reviewed retrospectively clinical records of 27 patients.

RESULTS: In our series, thirteen out of 21 patients (62%) were successfully treated and neurological development was normal on follow-up after embolization. In this same group of treated patients, four of the 21 (19%) showed improvement, but demonstrated permanent neurological disability. The mortality rate in our series was 24% (five out of 21 patients). These patient were all neonates presenting with severe cardiac failure and pulmonary hypertension, two of the infants presented with hemorrhagic complication before embolization, indicating a score below eight on the neonatal evaluation score by the Bicetre team, which would have placed these infants outside the indication. One patient demonstrated technical failure, representing our earlier clinical experience resulted in death.

CONCLUSION: In the absence of the brain damage on CT or MRI, urgent endovascular intervention should be indicated even if in GVM with severe congestive heart failure, pulmonary hypertension, evidence of arterial steal and central hypoxia.

Abstract No.12

Quantitative Digital Subtractive Angiography of Brain Vascular Disorders: Initial Experience

WY GUO, CJ LIN, ASZ HUNG, FC CHANG, CB LUO, JF LIN, WF CHU

Department of Radiology, Neurological Institute Neurosurgery, Taipei Veterans General Hospital;

School of Medicine, National Yang-Ming University, Taipei, Taiwan

BACKGROUND and OBJECTIVE: Quantitative digital subtractive x-ray angiography minimizes cross-devices, -patients, -time and -observers varieties. The current work was made to illustrate our initial experience of quantifying intracranial vascular circulation time, defined as the time of maximal intensity (Tmax, sec), in 305 patients with various brain vascular disorders.

METHODS: 305 patients with various brain vascular disorders that necessitated x-ray angiography for diagnostic/therapeutic purposes were recruited for post-processing using syngo iFlow(r) software (version VB15, Siemens Healthcare). Tmax at selected angiographic regions of interest of cases with normal appearing hemodynamics and various brain vascular disorders were determined, quantitatively. They were sub-classified as: no Tmax changes (as control group), delayed or prompted Tmax (as disease group) secondary to arteriovenous malformations/fistulae, moyamoya disease, arterial stenosis and aneurysm. For those receiving re-vascular or de-vascular procedures, the therapeutic effects were, quantitatively, defined according to the changes of Tmax.

RESULTS: For the control group, the Tmax was consistent with the previously published data stemmed from conventional x-ray angiography. For disease group, the intracranial hemodynamic improvement towards normalization was quantitatively illustrated by iFlow-DSA. Intra-operative Doppler confirmed the peri-therapeutic hemodynamic improvement.

CONCLUSIONS: Intracranial circulation time is reliably quantified by the color-coded DSA using iFlow with Tmax method. Without extra irradiation dose, iFlow DSA provides add-on and in-room information for investigating intracranial hemodynamics. The quantitative analysis facilitates therapeutic strategy-taking and enables the evaluation of therapeutic effects in an objective manner. Tmax normalization is also evidenced by improving cerebral blood flow and blood volume maps obtained from Doppler and MR perfusion imaging. However, currently, it is not possible to directly obtain tissue perfusion maps from two-dimensional DSA imaging.



Abstract No.13

Ozonucleolysis in Cervical Disc Prolapse

UR Chaudhry, F. Rauf, S.K. Bhatti, M. Farooq

Department of Interventional Neuroradiology, Lahore General Hospital/Post Graduate Medical Institute, Lahore, Pakistan

BACKGROUND AND OBJECTIVES: Direct injection of ozone has been proven to be effective alternative to surgery for patients suffering from disc herniation in many centres around the world. We report our experience with ozonucleolysis between June 2005 to July 2011 with 1000 patients affected by pain cervical region (Bracehalga) due to disc herniation including of postoperative recurrence disc prolapsed.

MATERIALS AND METHODS: All these cases treated by intradiscal, or paravertabral oxygen - ozone injections. Patients age between 20 to 70 years underwent percutaneous ozoneuclealylsis. The procedure done under the angiofioursocopy with full aspectic technique. The ozone generator, essential component placed close to the patients. Simple 23G needle to 22G spinal needle, (quincke type point) were used to inject ozone under fluoroscopy. No premedication or anesthesia were given and the procedures were performed at an outpatient facility with short hospital stay after the treatment.

RESULTS: Among 1000 patients 700 patients were followed up for 5 months, 50% of the treated patients showed complete recovery with disappearance of symptoms. 25% of cases complaint of occasional episodes of pain neck and arms but no limitations of occupational activities - 15% of the cases showed in sufficient improvement - 5% cases no improvement and went for surgery 10% of the cases never turned up after the first visit.

CONCLUSIONS: In our experience, Ozone Gas Therapy in treatment of herniated disc has revolutionized the percutaneous approach to nerve root disease making it safer cheaper and easier to repeat than treatments currently in use. So oxygen ozone therapy should be 1st choice of treatment in cervical disc prolapse.

Abstract No.14

Patient's Radiation Doses during Implantation Stents in Carotid Artery the Problem of Long-Lasting Procedures

W. Majewski^a, M.G. Stanisic^a, M. Makalowski^b,
N. Majewska^c, M. A. Blaszk^d, R. Juszkat^c, K. Krasinski^a,

^aGeneral and Vascular Surgery, K. Marcinkowski University of Medical Sciences, Poznan, Poland.

^bDepartment of Neurodiology, K. Marcinkowski University of Medical Sciences, Poznan, Poland.

^cDepartment of Radiology, K. Marcinkowski University of Medical Sciences, Poznan, Poland.

^dUniversity of Warsaw, Faculty of Physics, Department of Biomedical Physics, Warsaw, Poland.

BACKGROUND: The main purpose of this study was to document the radiation doses to patient's during implantations stents in cardiac artery and discuss potential reason for prolongation of radiological procedure.

OBJECTIVE: Carotid stent implantation can be disturbed by many factors, which, in turn, lead to prolongation of the procedure time and thus increase the radiation dose that a patient and hospital personnel are exposed to patients.

MATERIALS AND METHODS: Fluoroscopy and exposure time, air kerma (AK) and dose area product (DAP) were analyzed during carotid arteries stenting from 160 patients were analysed retrospectively in regards to body mass index (BMI), percent of stenosis, cerebral protecting system use or no, difficult anatomy.

RESULTS: In 80% of the analyzed patients total air kerma was lower than 0.5 Gy and for 17% exceeded 0.5 Gy. For 3% of patients this value was higher than 1 Gy and the maximum obtained air kerma was 1.2 Gy. Mean total DAP value for this kind of treatment was 54 Gy cm². This is caused by the fact that total mean AK was high for the cohort analysed and reached 254 mGy. The mean AK (exposure) of patients with BMI within the range 25-29.9 and with BMI >30 were significantly increased compared to that of patients with BMI 18-24.9 ($p=0.00004$, $p=0.000001$). The mean FT of patients with stenosis within the range 80-89% and with 90-99% were significantly increased compared to that of patients with stenosis 70-79% ($p=0.00006$, $p=0.00002$).

CONCLUSION: Radiation dose obtained by patient during CAS, might be high and reach 1Gy. Arteries stenosis, BMI, difficult anatomy, necessity, rough maneuvers leading to vasospasm may prolong procedure time and raise the risk of radiation overdose especially The use of cerebral protection systems does not significantly increase the dose so it is recommended to use.



Abstract No.15

Ultrasound guided fine needle aspiration biopsy is useful in the evaluation of post-radiated lymph nodes in patients with oropharyngeal squamous cell carcinoma

Salmaan Ahmed M.D., Thinh Vu M.D., Komal Shah M.D., Ping Liu M.S.,
Erich Sturgis M.D., John Stewart M.D., Lawrence Ginsberg M.D

MD Anderson Cancer Center, Houston, Texas, USA

BACKGROUND: Most patients receiving chemoradiation for oropharyngeal squamous cell carcinoma are cured by this therapy, with a few requiring neck dissections for residual disease. Identifying patients that require surgery is a challenge.

OBJECTIVE: The purpose of our study is to assess the performance of ultrasound guided fine needle aspiration biopsy (US-FNA) in determining the presence or absence of viable tumor, as compared to surgical histology and follow-up as a gold standard.

MATERIALS AND METHODS: Consecutive patients receiving chemoradiation for oropharyngeal squamous cell carcinoma with subsequent US-FNA performed within 160 days following completion of radiation therapy were selected for review. Patients were referred for US-FNA based on equivocal/concerning findings on contrast enhanced CT and/or physical exam. FNA was performed under US guidance to exclude residual tumor, and results were categorized as positive (viable tumor) or negative (lymphoid tissue, treatment effect, non-viable necrotic tumor) by a cytopathologist. 12 patients went on to consolidation neck dissection, and the rest were followed for recurrence at the biopsy site. Mean/median follow-up was 22/21 months.

RESULTS: 58 patients met inclusion criteria at our institution between 2005 and 2008, with US-FNA performed between 41 and 153 days (mean=78, median=74) following completion of radiation therapy. A total of 69 lymph nodes were biopsied (47 unilateral, 11 bilateral).

Of the 69 lymph nodes biopsied, FNA results were positive in 7 patients and negative in 62. Of the 62 patients with a negative FNA, none had tumor at surgery/follow-up (NPV=100%). 4/7 patients with a positive FNA demonstrated tumor at surgery (PPV=57%), and 3/7 patients had no tumor at surgery/follow up.

CONCLUSIONS: US-FNA is useful in evaluating for residual viable tumor within neck lymph nodes following chemoradiation for oropharyngeal squamous cell carcinoma, and demonstrates a 100% NPV in our study (PPV was 57%). Our study is limited by the small number of true positives.



Abstract No.16

Early Experience using Flow Diverters, Silk[®] Artery Reconstruction Device, in Fusiform Aneurysms

**Ahmad Sobri Muda¹, Rozman Zakaria¹, Nur Yazmin Yaacob¹,
Zahiah Mohamed¹, Azizi Abu Bakar², Ahmad Faizal Ali³**

¹Radiology Department, Universiti Kebangsaan Malaysia Medical Centre, Kuala Lumpur.

²Neurosurgical Department, Universiti Kebangsaan Malaysia Medical Centre, Kuala Lumpur.

³Radiology Department, Universiti Malaysia Serawak, Kuching

We describe early experience using Flow Diverter Stent for fusiform and wide neck aneurysms in 6 patients. Four patients had ICA aneurysms, and 2 patients had bilateral vertebral artery aneurysms. We used total of 9 SILK [Balt Extrusion, Montmorency, France] artery reconstruction devices and combined with LEO+ stent in 2 cases as the scaffolding. We describe the patient selections, immediate angiographic findings, and early clinical and neuroimaging outcome.



Abstract No.17

Embolisation of Brain AVM using Detachable Tip Microcatheter

**Ahmad Sobri Muda¹, Rozman Zakaria¹, Nur Yazmin Yaacob¹,
Zahiah Mohamed¹, Azizi Abu Bakar², Khairul Azmi Abdul Kadir³**

¹*Image Guided Intervention Centre (iMAGIC), Universiti Kebangsaan Malaysia Medical Centre, Kuala Lumpur.*

²*Neurosurgical Department, Universiti Kebangsaan Malaysia Medical Centre, Kuala Lumpur.*

³*Radiology Department, Universiti Malaya Medical Centre, Kuala Lumpur*

We review our cases of brain AVM embolisation using detachable tip microcatheter for a period of 36 months from jan 2009 until june 2011. We have used 2 types of detachable tip microcatheter available in the market, namely SONIC [Balt Extrusion, Montmorency, France] and APOLLO [ev3, Irvine, Calif]. Both microcatheters have different choices of detachable tip length. We describe the selection of various detachable tip length, placement of tip and injection technique to optimize the advantage of using detachable tip microcatheter.



Abstract No.18

Embolization of Mandibular Facial AVM using Onyx

Joharuddin Md Kasim¹, Lau Jia Him¹, Ahmad Sobri Muda²

¹Radiology Department, Hospital Kuala Lumpur. ²Image Guided Intervention Centre (iMAGIC).

Universiti Kebangsaan Malaysia Medical Centre, Kuala Lumpur

We describe 3 cases of mandibular facial AVM who presented with haemorrhage following a simple dental procedure. Further evaluation revealed presence of mandibular facial AVM and further dental procedure become high risk of excessive bleeding especially tooth extraction. As surgical resection for mandibular AVM is major complicated procedure, endovascular become the preferable option.

Embolisation using Onyx enable us to achieve near complete occlusion of the nidus via only one feeder, even part of the nidus which is not supplied by the cannulated feeder, compared to hystoacryl glue where nidus occlusion will only follow the flow of the cannulated feeder. We illustrate the microcatheter choice, injection technique and the outcome. The main disadvantage is the cost of Onyx.



Abstract No.19

Embolization of Jugular Vein Extasia: A Case Report

**Arvin R¹, SI Yun¹, Aida AA¹, Noor Aida Mat Daud¹,
Zuhanis, Ropiah¹, Ahmad Sobri Muda²**

*¹Radiology Department, Hospital Sungai Buloh, Selangor. ²Radiology Department,
Universiti Kebangsaan Malaysia Medical Centre, Kuala Lumpur*

Jugular vein ectasia is uncommon. Typical it takes a benign course and rarely poses life-threatening complication. In most treated cases is for cosmetic reason. Previously surgical option is the mainstay of treatment where the dilated and redundant veins were ligated. Potential complication surgically includes injury to adjacent structures like carotid artery and nerves.

We report a case of jugular vein ectasia required treatment for cosmetic reason using endovascular technique. Embolisation provide less invasive option with more concrete evaluation of the venous drainage to determine the safeness if the venous ectasia is occluded.

We describe the imaging findings, strategy and techniques of endovascular treatment.



Abstract No.110

Brain AVM EEmbolization with Onyx

**Zuhanis¹, Lau Jia Him¹, Si Yun¹, Aida AA¹, Noor Aida Mat Daud¹,
Arvin R¹, Ropiah¹, Azmin Kass Rosman², Saiful Azli², Ahmad Sobri Muda³**

¹Radiology Department, Hospital Sungai Buloh, Selangor. ²Neurosurgery Department, Hospital Sungai Buloh, Selangor.

³Radiology Department, Universiti Kebangsaan Malaysia Medical Centre, Kuala Lumpur

We report the initial experience by using a new liquid embolic agent (Onyx) for embolization of brain arteriovenous malformations (AVMs). Between Jan 2010 and July 2011, 45 patients with brain AVMs were embolized with Onyx. Complete obliteration can be achieved in small AVMs. Large AVMs can be adequately reduced in size to be considered for surgical or radiosurgical treatment. Onyx is feasible and safe in the embolization of brain AVMs.



Abstract No.Y1

Utility of Skewness and Kurtosis Derived from MR Perfusion Histogram to Predict Pseudoprogression in Patients with Glioblastomas

H. J. Baek, M.D., H. S. Kim, M.D., H. Y. Lee, M.D., Y. J. Choi, M.D.

*Department of Radiology and Research Institute of Radiology,
University of Ulsan College of Medicine, Asan Medical Center, Seoul, Korea.*

BACKGROUND: The differentiation of tumor recurrence from pseudoprogression has a great importance for outcome evaluation in clinical practice. However, despite no single imaging technique has been validated to adequately establish a clear distinction between them.

OBJECTIVE: To semiquantitatively differentiate pseudoprogression from early tumor recurrence using both skewness and kurtosis derived from MR perfusion histogram.

METHODS: 135 patients with newly diagnosed glioblastomas underwent chemoradiotherapy (CCRT) after surgical resection. New or enlarged contrast-enhancing lesions after CCRT were prospectively assessed by dynamic susceptibility contrast-enhanced perfusion MR imaging. According to their histogram pattern of relative cerebral blood volume (CBV), study patients were classified into 4 groups: group 1, positive skewness and leptokurtic; group 2, positive skewness and platykurtic; group 3, negative skewness and leptokurtic; group 4, negative skewness and platykurtic. All patients were regularly followed up by conventional and perfusion MR images. Predictors for pseudoprogression were determined by logistic regression analysis.

RESULTS: After CCRT, new or enlarged contrast-enhancing lesions were found in 79 of 135 patients (58.5%), which were subsequently classified as pseudoprogression (37 patients, 27.4%) and early tumor recurrence (42 patients, 31.1%). Pseudoprogression were developed in 18 (75.0%) of 24 patients of group 1, in 7 (46.7%) of 15 patients of group 2, in 9 (45.0%) of 20 patients of group 3, and in 0 (0%) of 20 patients of group 4, respectively (Chi-square test, $P < 0.0001$). The receiver operating characteristic (ROC) curve-derived threshold value (groups 1 and 2) differentiated pseudoprogression from early tumor recurrence with a sensitivity of 89.2% and a specificity of 85.7%. Histogram pattern (skewness and kurtosis) of relative CBV was a independent predictor for pseudoprogression (Odds ratio 9.11 [3.18 - 26.07], $P < 0.0001$).

CONCLUSION: Semiquantitative histogram pattern analysis of relative CBV with both skewness and kurtosis may be a promising approach to differentiate pseudoprogression from early tumor recurrence in patients with posttreatment glioblastomas.

Abstract No.Y2

Metal Artifacts Reduction for Lumbar Spine Computed Tomography by Various Image Acquisition Parameters

Titipong Kaewlek¹, Diew Koolpiruck², Saowapak Thongvigitmanee³, Manus Mongkolsuk⁴,
Sastrawut Thammakittiphan⁵, Monchai Ruangchainikom⁶, Pipat Chiewvit⁷.

¹Biological Engineering Program, ²Department of Control Systems and Instrumentation Engineering, Faculty of Engineering, King Mongkut's University of Technology Thonburi, Bangkok; ³National Electronics and Computer Technology Center, Pathumthani; ⁴Department of Radiological Technology, Faculty of Medical Technology, Mahidol University, Nakhon Pathom; ^{5,7}Siriraj Imaging Center, Division of Diagnostic Radiology, Department of Radiology, ⁶Department of Orthopedic Surgery, Faculty of Medicine, Siriraj Hospital, Mahidol University, Bangkok, Thailand.

BACKGROUND: The metallic artifacts generated from computed tomography in case of metal implants embedded in a patient body may cause incorrect diagnosis. We try to reduce metal artifacts for improve detail of computed tomography imaging by various tube voltage, tube current and slice thickness setting.

OBJECTIVES: To study the effect of adjustment image acquisition parameter for reducing metal artifacts in lumbar spine imaging.

MATERIALS AND METHODS: The Catphan phantom and attached pedicle screws were used at the right, left, top and bottom of the phantom to generate the lumbar spine imaging with metal artifacts in the spine protocol the sizes of pedicle screw, including 0.55, 0.65, 0.75, and 0.85 mm in diameter. For image acquisition, tube voltage, tube current, and slice thickness were varied from the standard protocol while fixing other parameters. Evaluation of image quality was performed in term of noise and high resolution (Modulation Transfer Function: MTF), as well as of radiation dose (Computed Tomography Dose Index Volume: CTDIvol).

RESULTS: The results found that metal artifacts increased according to the size of pedicle screw. However, increasing tube voltage, tube current, and slice thickness from standard protocol (120 kV, 320 mA, 0.625 mm), metal artifacts decreased. By increasing the tube voltage, tube current, and thickness, the standard deviation of noise is decreased; For example, the noise is equal to 49.84 for 120 kV, 320 mA, 0.625 mm, and 32.75 for 140 kV, 500 mA, 0.625 mm. For the setting of 120 kV, 320 mA, 0.625 mm, the 50% MTF is equal to 2.96, and for the setting of 140 kV, 320 mA, 0.625 mm, the 50% MTF is equal to 3.89. Increasing the tube current and tube voltage, cause higher radiation dose, i.e., CTDIvol is equal to 16.11 mGy (120 kV, 320 mA, 0.625 mm) and 35.24 mGy (140 kV, 500 mA, 0.625 mm).

CONCLUSION: The presence of metal artifacts was scanned by the standard protocol. A large screw size has more metal artifacts more than a smaller screw size. The method of tube voltage and tube current adjustment could be used to reduce metal artifacts and improve image quality but with an increasing in radiation dose by 2.19 times (16.11 -35.24 mGy). Radiation dose equal to 35.24 mGy is acceptable since the limitation in ICRP is 50mGy/year, this amount does not the threshold dose on nearly critical organs such as ovary or testicle.

*Abstract No.Y3*

Highly Prominent Red Nuclei Lesions in Metronidazole-Induced Encephalopathy

Pattamon Panyakaew¹, Nath Pasutharnchat¹, Sasitorn Petcharunpaisan²

¹*Division of Neuroradiology, Department of Medicine, Faculty of Medicine, Chulalongkorn University, Bangkok, Thailand.*

²*Division of Diagnostic Radiology, Department of Radiology, King Chulalongkorn Memorial Hospital, Thai Red Cross Society, Bangkok, Thailand.*

BACKGROUND: The most favorite target of Metronidazole-induced encephalopathy (MIE) is cerebellar dentate nuclei. Symmetrical lesions affecting brainstem nuclei and splenium of corpus calosum have also been described. Infrequently, red nucleus and subthalamic nuclei may be involved. Lesions are usually reversible after discontinuation of metronidazole. Mechanism of MIE is not well understood, but it is thought to be related to neurotoxicity.

OBJECTIVE: To report a unique case of MIE prominently symmetrically involved red nuclei.

METHODS: The authors reported a 62-year-old woman who underwent Whipple's operation for advanced carcinoma of ampulla of Vater. Oral metronidazole at the dose of 1.5 g/day had been administered for 2 months for the intra-abdominal infection before she developed subacute onset of truncal ataxia and dysarthria. Neurological examination revealed symmetrical dysmetria, gait ataxia and scanning speech.

RESULTS: Magnetic resonance imaging (MRI) of the brain showed very prominent hyperintense lesions on T2-weighted and fluid-attenuated inversion recovery (FLAIR) images symmetrically involved the red nuclei. Hyperintense lesions also involved cerebellar dentate nuclei, superior olivary nuclei, dorsal medulla and splenium of corpus callosum. Diffusion-weighted images (DWI) showed restricted fluid diffusion of the lesion only at corpus callosum. Diagnosis of MIE was made, based on history and characteristic MRI findings. After discontinuation of metronidazole, the symptoms gradually resolved.

CONCLUSION: The authors reported a case of MIE with very striking, huge and round red nuclei lesions on FLAIR images. The most prominent target in MIE may be varied among cases. Selective involvement of the grey matters may suggest that MIE is possibly related to an energy failure.

Abstract No.Y4

MRI of Thai Patients with Positive Anti-AQP4 Antibody

Waraporn Pienpuck, Orasa Chawalparit,
Pornpong Jitpratoom, Sasitorn Siritho, Naraporn Prayoonwiwat

Faculty of Medicine Siriraj Hospital, Mahidol University, Bangkok, Thailand.

OBJECTIVE: To study the characteristics of MRI findings in Thai patients with positive serum aquaporin-4 antibody.

MATERIAL AND METHOD: Fifty-three Thai patients attending Siriraj MS clinics with positive anti-AQP4 antibody were retrospectively study. The available brain and spinal MRI in the hospital archive system were reviewed by two neuroradiologists and finalized by consensus. Clinical data and MRI findings were analyzed.

RESULTS: Thirty-three cases with available MRI were included. There were 32 brain MRI and 27 spinal MRI (26 with brain MRI) for the analysis. The mean age of the patients was 42.7 years old (range 17-81) with 31 females. Clinical diagnosis was made in 9 cases of NMO, 8 high risk NMOS, 5 RRMS, 1 PPMS, 1 PRMS, 1 OSMS and 2 Sjogren disease. There were 5 inconclusive diagnostic cases at the time data analysis. The time from attack to imaging study was varied from 1 day to 5 years. Thirteen cases had follow up MRI mostly more than 3 months interval. For Brain MRI, 50% were fulfilled Barkhof's criteria, 25% involved corpus callosum, 12.5% had brain atrophy and 15.6% had negative findings. Nodular pattern of T2 lesions were found in most cases and 13 cases (40.6%) had only nodular lesions. The remaining 43.7% had either confluent, patchy, or mixed pattern of T2 lesions. The involvement of brain in common location of AQP-4 were found: subependymal third/fourth ventricle (37.5%), subependymal lateral ventricle (28.1%), and medullar extending to cervical cord (18.8%). Extensive hemispheric lesion and corticospinal tract lesion were found in 12.5% and 15.6% respectively. There was 43.8% with nonspecific pattern. Most of the lesions had cloud-like enhancement and vasogenic edema. For spinal cord MRI, gadolinium enhancement was not performed in one case. Negative finding was found in 4 cases (14.8%) and positive in 23 cases (85.2%). Among the positive cases, 47.8% had one T2 lesion and 52.2% had more than one lesion, mostly at thoracic level. There were 15 cases (57.7%) with enhancing lesions, 5 cases (18.5%) with cord swelling, 18 cases (66.7%) with long extensive lesion (more than 3 vertebral body), 13 cases (48.1%) with central cord location on axial plane, 5 cases (21.3%) with peripheral location, and 5 cases (21.3%) with mixed pattern. When comparing Barkhof's brain criteria with spinal cord lesion, no significant difference was found between patients with fulfilled and not fulfilled the criteria. There was significant association of brain located AQP4 lesion and clinical diagnosis ($p < 0.05$). No association was found between length of spinal cord lesion and brain located AQP4 lesion.

CONCLUSION: The MRI findings of Thai patients with positive anti-AQP4 antibody had high incidence of brain lesion along the located AQP4 and long extensive cord lesion as other Asian countries.



Abstract No.Y5

Magnetic Resonance Imaging Appearances of Hypothalamic Lesions in Children - A Pictorial Essay

Penukonda SL¹, .Tang P H¹. Chan D²

¹*Department of Diagnostic Imaging, KK Women's and Children's Hospital, Singapore*

²*Department of Pediatric Medicine, KK Women's and Children's Hospital, Singapore*

BACKGROUND: Hypothalamic lesions constitute important childhood brain lesions. Hypothalamus may be affected by primary lesions or may be involved secondarily by various lesions from adjacent structures. Primary lesions can be neoplastic lesions like gliomas, congenital lesions like hamartomas or inflammatory lesions. MRI is the best modality to evaluate these lesions.

OBJECTIVE: To demonstrate various MRI appearances of hypothalamic lesions seen in childhood.

METHODS: A retrospective review of MR brain imaging reports performed in our hospital for a period of 2 years from January 2009 to January 2011 was done for all children presenting with hypothalamic symptoms. The MR reports were reviewed and those with positive MR findings in the hypothalamus were included in the study.

RESULTS: Out of total 1800 brain MRIs performed during this period, 98 children presented with hypothalamic symptoms like precocious puberty, diabetes insipidus and gelastic seizures etc. Out of these 40 patients showed hypothalamic lesions. Three children were presenting for some other symptoms (drowsiness, left sixth nerve palsy and nystagmus) and the hypothalamic lesions were found incidentally.

There were 22 opticochiasmatic hypothalamic gliomas, 7 hamartomas, 7 germinomas, 1 osteolipoma, 1 metastasis and 5 suprasellar masses which involved the hypothalamus.

CONCLUSION: MRI is helpful in defining the origin and extent of the hypothalamic lesions and signal characteristics can point to the diagnosis.

Abstract No.Y6

Value of Diffusion Tensor Imaging in Differentiating Low-Grade from High-Grade Gliomas: Preliminary Data

Siriwan Piyapittayanan, MD¹, Orasa Chawalparit, MD¹, Tumtip Sangruchi, MD²,
Theerapol Witthiwej³, MD, Sith Sathornsumetee⁴, MD, Sarun Nunta-aree, MD³

¹Department of Radiology, ²Department of Pathology, ³Department of Surgery, ⁴Department of Medicine (Neurology).

Faculty of Medicine Siriraj Hospital, Mahidol University, Bangkok, Thailand.

BACKGROUND: The prognosis and management are different between low grade and high grade cerebral gliomas. Despite optimization of sequences and protocols, preoperative grading of gliomas with conventional MRI (cMRI) is sometimes unreliable. Diffusion tensor imaging (DTI) give information about water mobility and tissue microstructure and organization in relation to directionality of diffusion.

OBJECTIVE: To determine the usefulness of DTI in differentiating low grade from high grade gliomas.

METHODS: Eighteen patients with cerebral gliomas underwent cMRI and diffusion tensor MR imaging before surgery. All patient have pathologically proven cerebral gliomas, who were classified into two groups, i.e. 11 patients with high grade gliomas (8 glioblastoma multiforme and 3 anaplastic astrocytoma), and 7 patients with low grade glioma (3 oligodendroglioma, 2 diffuse astrocytoma, 1 astrocytoma and 1 chordoid glioma). We measured FA and ADC values in regions of interest including enhancing area/non-enhancing area (if tumors do not enhance), necrotic area, peritumoral high T2 area, contralateral normal appearing white matter (NAWM) and normal corpus callosum. Pairwise comparisons were performed by using the ANOVA test.

RESULTS: The mean ADC value in high grade glioma was highest in necrotic area ($2.159 \pm 0.806 \times 10^{-3} \text{ mm}^2/\text{sec}$), followed by peritumoral high T2 area ($1.330 \pm 0.194 \times 10^{-3} \text{ mm}^2/\text{sec}$), enhancing area ($1.122 \pm 0.189 \times 10^{-3} \text{ mm}^2/\text{sec}$), normal corpus callosum ($0.789 \pm 0.055 \times 10^{-3} \text{ mm}^2/\text{sec}$) and contralateral NAWM ($0.768 \pm 0.041 \times 10^{-3} \text{ mm}^2/\text{sec}$). The mean FA value in high grade glioma was highest in normal corpus callosum (0.751 ± 0.053) and lowest in necrotic core (0.125 ± 0.046). The mean ADC value in low grade glioma was highest in necrotic area ($2.351 \pm 0.000 \times 10^{-3} \text{ mm}^2/\text{sec}$), followed by enhancing area ($1.484 \pm 0.495 \times 10^{-3} \text{ mm}^2/\text{sec}$), peritumoral high T2 area ($1.300 \pm 0.191 \times 10^{-3} \text{ mm}^2/\text{sec}$) and contralateral NAWM ($0.775 \pm 0.041 \times 10^{-3} \text{ mm}^2/\text{sec}$). The mean FA value in low grade glioma was highest in normal corpus callosum (0.781 ± 0.071) and lowest in enhancing area (0.135 ± 0.062). The only ADC value in enhancing tumor area was significantly different between high grade glioma and low grade glioma, $P = 0.042$.

CONCLUSION: Only ADC value in enhancing tumor area can be used to differentiate high grade glioma and low grade glioma.



Abstract No.Y7

Salivary Gland Tumours and Tumour like Lesions: Multi-modality Imaging Features and Histopathological Correlation

Y.T. Huang¹, A. Lam², S.S. Bhuta^{1,3}

¹Department of Medical Imaging, Gold Coast Hospital, Queensland, Australia

²Department of Pathology, Gold Coast Hospital, Queensland, Australia

³School of Medicine, Griffith University, Australia

BACKGROUND: Salivary gland neoplasms are relatively rare. Most of them are benign (70-80%) and found in the parotid glands (80-90%). Major salivary gland tumours often presents with an enlarging mass but not uncommonly, are identified incidentally. Imaging of salivary gland is multi-modality with ultrasound (US) and computed tomography (CT) as first-line for diagnosis. Magnetic resonance imaging (MRI) is often useful in specifying the diagnosis, operative planning and understanding tumour relationship with the facial nerve and its invasion (perineural spread). Apparent Diffusion Coefficient (ADC) values can be used to differentiate benign and malignant tumours.

OBJECTIVE: To describe typical imaging findings of common benign and malignant tumours of the major salivary glands. Tumour-like lesions are also reviewed as while are uncommon, often results in diagnostic pitfalls.

METHOD: Retrospective review of cases referred from specialist Head and Neck clinic was performed. Patients were imaged with US, 128 slice multi-detector CT and 1.5T MRI as required and radiologic diagnoses were correlated biopsy and/or post operative histopathology. Findings are presented as a pictorial review.

RESULTS: The characteristic imaging (US/CT/MRI) appearances of the common types of salivary gland neoplasms including pleomorphic adenoma (benign mixed tumour), Warthin, mucoepidermoid carcinoma, adenoid cystic carcinoma, squamous cell carcinoma, lymphoma and metastases are highlighted. Tumour-like lesions such as lipoma, cysts, Kutners tumour and schwannomas are also included as part of this comprehensive educational exhibit of major salivary gland imaging. Clinical correlation was performed for all lesions and confirmed with histopathology (histopathological images are included where available).

CONCLUSION: Salivary gland tumours remain a diagnostic challenge for radiologists due to variety of differential diagnoses including an array of mimicking tumour-like lesions. Multi-modality imaging especially with MRI can add diagnostic specificity and narrow the differential diagnosis. A broad understanding of the common pathological types, key radiological finding is essential to avoid pitfalls.

Abstract No.Y8

Utility of Skewness and Kurtosis Derived from MR Perfusion Histogram to Predict Progression-free Survival in Patients with Newly Diagnosed Glioblastomas

JW Park, CG Choi, SJ Kim, DC Suh, HS Kim

*Department of Radiology and Research Institute of Radiology, University of Ulsan College of Medicine,
Asan Medical Center, Seoul, Korea*

BACKGROUND: Dynamic susceptibility weighted contrast-enhanced (DSC) MR imaging provide a means of characterizing tumor biology. The effectiveness of histogram analysis of relative cerebral blood volume (CBV) values for glioma grading is known to reflect heterogeneous tumor vascularity in high-grade gliomas.

OBJECTIVE: To retrospectively determine whether skewness and kurtosis derived from relative CBV histogram can be used to predict progression-free survival in patients with newly diagnosed glioblastoma.

MATERIALS AND METHODS: 121 patients (72 male and 49 female patients; mean age, 49 years) were examined with DSC perfusion MR imaging and were followed up clinically with MR imaging (mean follow-up, 19 weeks). Subanalyses were performed by stratifying the population according to their histogram pattern: group 1, positive skewness and leptokurtic; group 2, positive skewness and platykurtic; group 3, negative skewness and leptokurtic; group 4, negative skewness and platykurtic. The differences in progression-free survival and overall survival between subgroups were calculated with the Kaplan-Meier method. Cox proportional hazards regression was used to determine whether age, sex, resectability, tumor size and relative CBV were associated with an adverse event.

RESULTS: Kaplan-Meier estimates of median time to progression in weeks indicated that patients of group 1, 2, 3, and 4 had a median time to progression of 47, 21, 14, and 13 weeks, respectively ($P = 0.0005$). Median overall survival for the group 1, 2, 3, and 4 were 62, 57, 55, and 52 weeks, respectively ($P = 0.0532$). Skewness and kurtosis of relative CBV was the most strongest independent predictor of progression-free survival.



Platinum Sponsors

Toshiba

Philips

Gold Sponsors

Pacific Healthcare

EV3

Johnson & Johnson

Siemens

Bayer Healthcare

Other Sponsors

Fuji

QE Healthcare

BJC

BRACCO

Lippincott Williams & Wilkins

Asahi Intecc

Boston Scientific



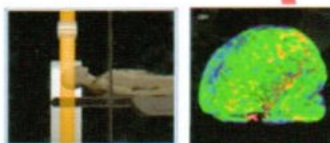
The World's First Dynamic Volume CT

640 Slices 4 Dimensions CT scanner

ONE Rotation

The wide coverage provided by the 160 mm-wide Area Detector enables scanning of the heart or brain within one rotation, eliminating the need for helical scanning.

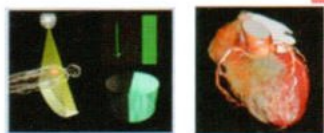
An entire organ can be captured at one time, resulting in multiplanar and 3D images demonstrating perfect continuity along the Z-axis. In addition, ultrafast scan times allow the contrast medium dose and exposure dose to be reduced.



Whole brain Perfusion

ONE Phase

The entire heart can be captured in as little as one rotation for coronary analysis, or over a single heartbeat to include complete functional diagnosis.



Whole heart image

Each reconstructed 3D volume represents exactly the same phase the cardiac cycle, providing incredible motion-free images of the coronary arteries with homogenous contrast enhancement.

ONE Volume

The ability to acquire the entire brain with one volume scan opens the door to new diagnostic possibilities.

The Neuro ONE protocol allows acquisition of multiple low-dose volume scans of the entire brain during contrast infusion to provide whole brain perfusion and whole brain dynamic vascular analysis in one examination. Dynamic volumetric acquisition protocols can also be used to review moving joint structures in 3D, providing new clinical applications in orthopedic imaging.



Whole body Image

Ultrasound System

Precision Precision Imaging technology increases productivity and diagnostic confidence by providing more detailed ultrasound images. As a multi-resolution signal processing technology, it not only evaluates images line-by-line, but also includes information from adjacent lines to enhance the amount of information obtained.

Differential Tissue Harmonic technology provides 2D images of unsurpassed spatial resolution and contrast, along with greatly increased penetration.

ApliPure™ real-time compounding delivers 2D images of outstanding clarity and detail in all modes, while preserving clinically significant markers.

Advanced Dynamic Flow™ adds superior spatial resolution to color Doppler to reveal minute vasculature with unprecedented accuracy and detail.

3D/4D extends your diagnostic capabilities into the next dimension of imaging and intervention by providing accurate renderings and arbitrary volume cuts in real time or offline.

With full **DICOM** connectivity and IHE compliance, Aplio XG integrates seamlessly into all kinds of networked clinical environments.

MicroPure is microcalcification detection technology for distinguish small calcification from breast tissue.



CMC Biotech CO., LTD.

364 Muban Town-in-Town, Soi Ladphrao 94, Ladphrao Road, Wangthonglang, Bangkok 10310

Marketing & Sales Department: Tel. +66(0)2530-4995 Fax. +66(0)2935-6527

Service Department: Tel. +66(0)2935-6667-8 (24 Hours)

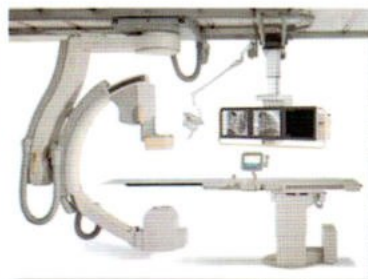
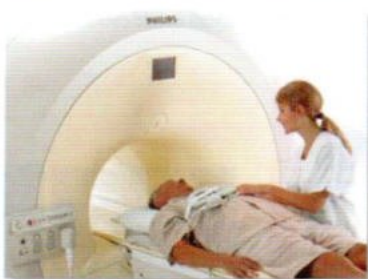
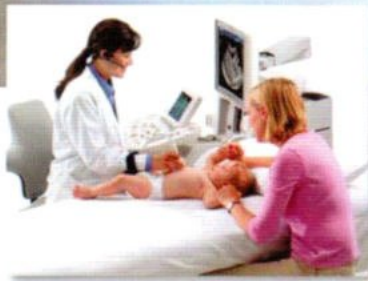
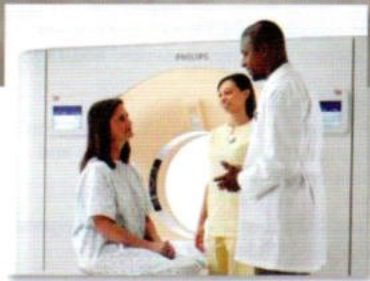
Northern Branch: Tel. +66(0)5328-3261 Fax. +66(0)5320-4463

North Eastern Branch: Tel. +66(0)4334-1642 Fax. +66(0)4334-1643

Southern Branch: Tel. +66(0)7442-9803 Fax. +66(0)7442-9804



TOSHIBA
Leading Innovation >>>



Philips Electronics (Thailand) Ltd.

28th floor, Thai Summit Tower New Petchburi Road,
Khwang Bangkok Khet Huaykhwang Bangkok 10310

Tel. 02-614 3440 Fax. 02-614 3562

www.philips.com

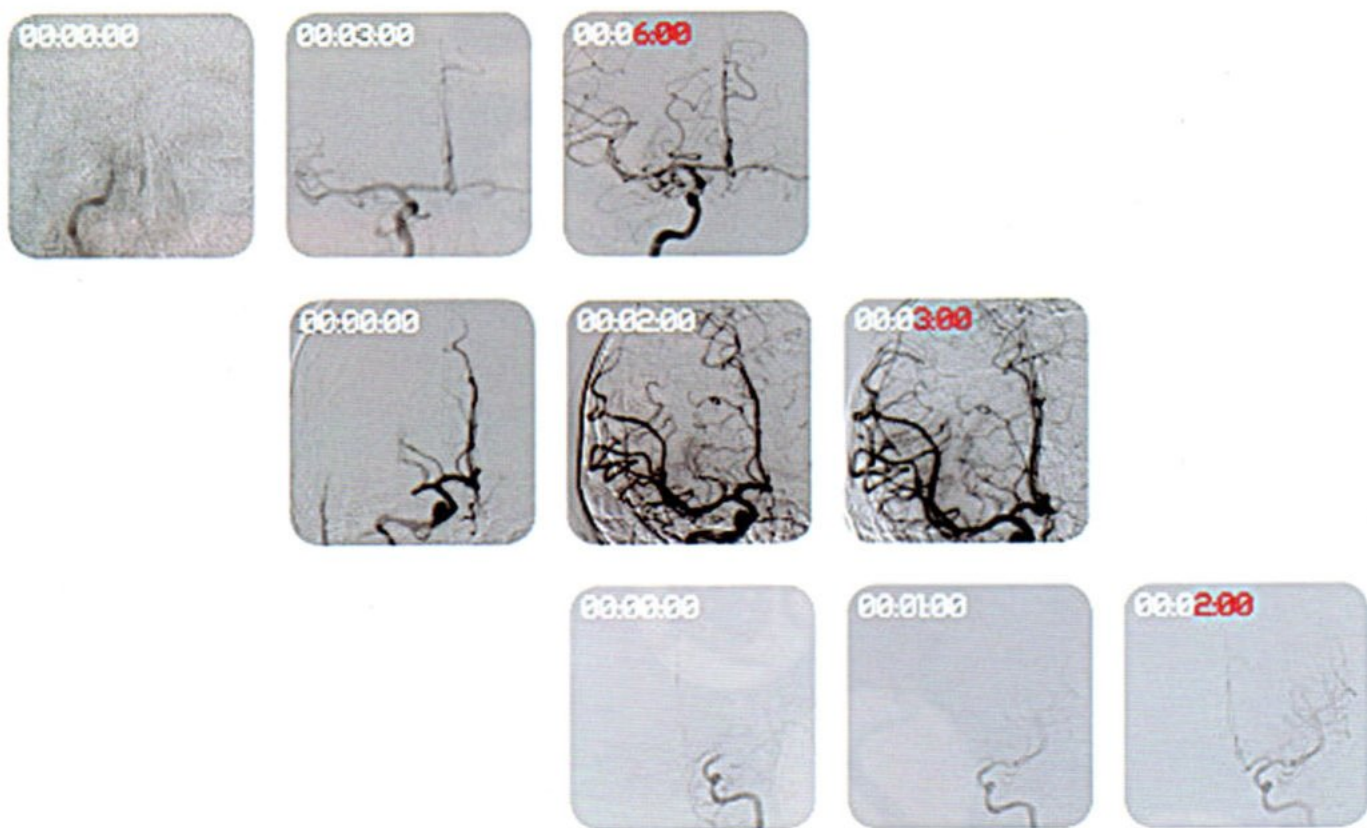
PHILIPS

sense and simplicity

Penumbra System® 054

FRONTLINE

SPEED and *VERSATILITY*



Credits for images, from top to bottom: Dr. Jeff Parkas, Maimonides Medical Center, Brooklyn, NY; Dr. Reza Jahan, UCLA, Los Angeles, CA; and Dr. Chris Baker, Maine Medical Center, Portland, ME.

Penumbra 

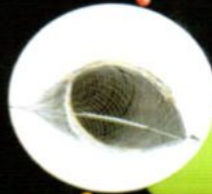


บริษัท แปซิฟิก เฮลท์แคร์ (ไทยแลนด์) จำกัด

1011 อาคารสุภาลัย แกรนด์ ทาวเวอร์ ห้อง 01 ชั้น 29 ถนนพระราม 3 แขวงคลองตันใต้ เขตวัฒนา กรุงเทพฯ 10120
Tel. (66 2) 881-2488 Fax. (66 2) 683 3373 www.phc.co.th



Solitaire Revascularization Device



SpiderFX Embolic Protection Device



Rebar 18 Reinforced Micro Catheter



Pipeline Embolisation Device



ONYX Liquid Embolic System



Mirage Hydrophilic Guide Wire



Axiom Detachable Coil



Forecast Science Consultant Co., Ltd.

11/26 Kanjanapisek Rd, Sao-Tonghin, Bangyai, Nontaburi, 11140

Tel : 02-9678081 , 02-9248183 Fax : 02-9678086 www.forecastscience.com

S E E K & F E E L T H E D I F F E R E N C E

Orbit GALAXY™
DETACHABLE COIL SYSTEM

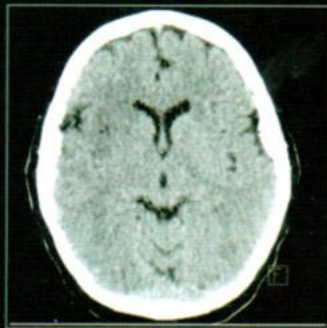


never stop moving™

Codman
a Johnson & Johnson company
NEUROVASCULAR

Complete Stroke Protocol

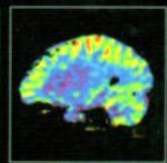
Non-enhanced CT scan



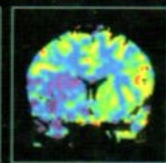
Arterial phase MIP



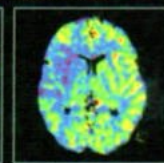
Perfused blood volume reconstruction - sagittal



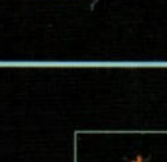
Perfused blood volume reconstruction - coronal



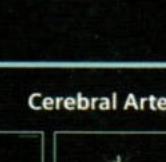
Perfused blood volume reconstruction - axial



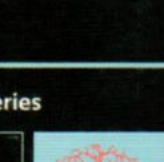
Perfusion CT Cerebral blood flow



Perfusion CT Cerebral blood volume



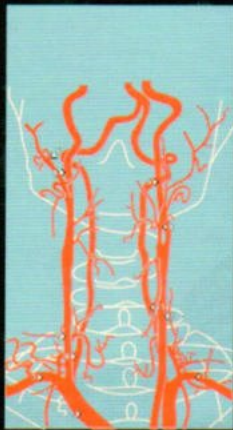
Perfusion CT Time to peak



References

8. F. Tonndorf, F. Klotz, R. Handke, et al. Comprehensive imaging of ischemic stroke with multislice CT. *Radiographics* 2003; 23: 565-592 [5]. P. Klotz, F. Klotz, D. G. Nabel, et al. Color-coded perfused blood volume imaging using multidetector CT: initial results of whole-brain perfusion analysis in acute cerebral ischemia. *Eur Radiol* 2007; 17: 2352-2358

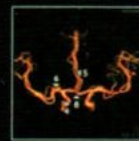
Cervical Arteries



1. Brachiocephalic trunk
2. Right common carotid artery
3. Right subclavian artery
4. Right vertebral artery
5. Right external carotid artery
6. Right internal carotid artery
7. Left common carotid artery
8. Left external carotid artery

9. Left internal carotid artery
10. Left subclavian artery
11. Left vertebral artery

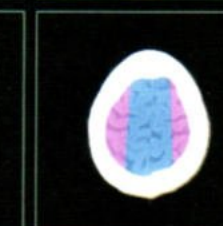
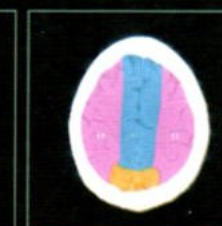
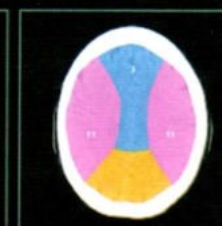
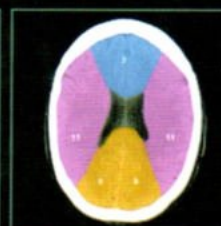
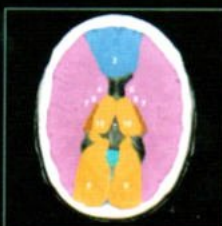
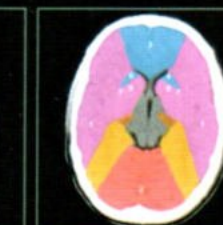
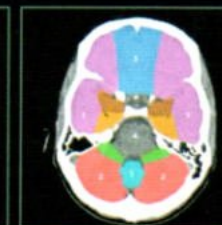
Cerebral Arteries



1. Basilar artery
- 2a. Right posterior cerebral artery
- 2b. Left posterior cerebral artery
- 3a. Right superior cerebellar artery
- 3b. Left superior cerebellar artery
4. Internal carotid artery

5. Anterior cerebral artery
6. Middle cerebral artery
7. Left posterior communicating artery
8. Anterior communicating artery

Arterial Vascular Territories



- Middle cerebral artery ■ Posterior cerebral artery ■ Anterior cerebral artery ■ Posterior inferior cerebellar artery ■ Anterior inferior cerebellar artery ■ Superior cerebellar artery ■ Anterior choroidal artery

1. Temporal lobe
2. Cerebellum
3. Frontal lobe
4. Pons
5. Cerebellar vermis
6. Caudate nucleus
7. Lentiform nucleus
8. Internal capsule
9. Occipital lobe
10. Thalamus
11. Parietal lobe

CT Neuro Anatomy and Pathology

Answers for life.

SIEMENS

CT images from SOMATOM Sensation 64 slice configuration and SOMATOM Definition using CT Neuro Engine. Courtesy of University of Munich-Groenenhagen Campus, Munich, Germany and courtesy of the Department of Clinical Radiology, University Hospital Witten, Germany.



Enhancing Diagnosis. Empowering Care.



Bayer HealthCare

FUJIFILM



Wolters Kluwer
Health

Lippincott
Williams & Wilkins



**Boston
Scientific**
Defining tomorrow, today.™

